Received: 27 January 2022 | Accepted: 18 December 2022

DOI: 10.1111/pce.14522

ORIGINAL ARTICLE

Plant, Cell & Environment | WILEY

Multispecies comparison of host responses to *Fusarium circinatum* challenge in tropical pines show consistency in resistance mechanisms

Erik A. Visser[1] | Tamanique P. Kampmann[1] | Jill L. Wegrzyn[2] | Sanushka Naidoo[1]

[1]Department of Biochemistry, Genetics and Microbiology, Forestry and Agricultural Biotechnology Institute (FABI), University of Pretoria, Pretoria, South Africa

[2]Department of Ecology and Evolutionary Biology, University of Connecticut, Storrs, Connecticut, USA

Correspondence

Sanushka Naidoo, Department of Biochemistry, Genetics and Microbiology, Forestry and Agricultural Biotechnology Institute (FABI), University of Pretoria, Pretoria, South Africa.
Email: sanushka.naidoo@fabi.up.ac.za

Funding information

Department of Science and Innovation (DSI), South Africa, Technology Innovation Agency (TIA), Forest Molecular Genetics cluster programme

Abstract

Fusarium circinatum poses a threat to both commercial and natural pine forests. Large variation in host resistance exists between species, with many economically important species being susceptible. Development of resistant genotypes could be expedited and optimised by investigating the molecular mechanisms underlying host resistance and susceptibility as well as increasing the available genetic resources. RNA-seq data, from *F. circinatum* inoculated and mock-inoculated ca. 6-month-old shoot tissue at 3- and 7-days postinoculation, was generated for three commercially important tropical pines, *Pinus oocarpa*, *Pinus maximinoi* and *Pinus greggii*. De novo transcriptomes were assembled and used to investigate the NLR and PR gene content within available pine references. Host responses to *F. circinatum* challenge were investigated in *P. oocarpa* (resistant) and *P. greggii* (susceptible), in comparison to previously generated expression profiles from *Pinus tecunumanii* (resistant) and *Pinus patula* (susceptible). Expression results indicated crosstalk between induced salicylate, jasmonate and ethylene signalling is involved in host resistance and compromised in susceptible hosts. Additionally, higher constitutive expression of sulfur metabolism and flavonoid biosynthesis in resistant hosts suggest involvement of these metabolites in resistance.

KEYWORDS

host-pathogen interaction, *Pinus greggii*, *Pinus maximinoi*, *Pinus oocarpa*, *Pinus patula*, *Pinus tecunumanii*, transcriptome assembly

1 | INTRODUCTION

A notable threat to forestry around the world is the fungal pathogen *Fusarium circinatum* (Nirenberg & O'Donnell, 1998), which can affect more than 60 species of *Pinus*, causing pitch canker in mature trees and a wilting disease in seedlings (Crous, 2005; Gordon et al., 2001; Mitchell et al., 2011; M. J. Wingfield et al., 2008). Since the first description of the disease in the south-eastern United States (Hepting & Roth, 1946), *F. circinatum* has spread to multiple countries (Gordon et al., 2015; Vettraino et al., 2018), resulting in significant losses to industry (Mitchell et al., 2011; M. J. Wingfield et al., 2008) and natural populations of susceptible species such as *Pinus radiata* (Earle, 2022).

Many commercially important *Pinus* species, such as *Pinus greggii*, *Pinus patula* and *Pinus radiata* are highly susceptible to *F. circinatum* challenge (Hodge & Dvorak, 2000). Current short-term management strategies mainly focus on increased silvicultural hygiene to limit

spread of the pathogen in affected areas and prevent spread to unaffected areas (Gordon et al., 2015). Long-term control strategies aim to incorporate genetic resistance of less susceptible species, such as *Pinus maximinoi*, *Pinus oocarpa* and low elevation provenances (LE) of *Pinus tecunumanii*, either through direct usage of alternative species or production of hybrids between resistant species and more susceptible species with desirable wood and growth traits (Dvorak, 2012; Gordon et al., 2015; Mitchell et al., 2011).

Our knowledge of the genetic and molecular mechanisms underlying this plant-pathogen interaction is growing rapidly. Past studies aimed at identifying genes or genomic loci involved in the interaction between *Pinus* spp. and *F. circinatum* relied on marker-based methods (Donoso et al., 2015; Moraga-Suazo et al., 2014; Morse et al., 2004; Quesada et al., 2010). More recent studies provided the first global views of these interactions through dual RNA-sequencing and proteomics of the pathogen and various pine hosts (Amaral et al., 2021; Carrasco et al., 2017; Hernandez-Escribano et al., 2020; Visser et al., 2019; Zamora-Ballesteros et al., 2021).

Plant defences are broadly categorised as constitutive and induced. Constitutive defences include physical, such as cell walls and bark, as well as chemical, such as oleoresin and phytoanticipins, barriers that protect against pathogen and pest attack (Nurnberger & Kemmerling, 2009; Nürnberger & Lipka, 2005). Recent studies on host resistance to *F. circinatum* challenge in pines have focused on induced responses following pathogen challenge (Amaral et al., 2021; Carrasco et al., 2017; Hernandez-Escribano et al., 2020; Visser et al., 2019; Zamora-Ballesteros et al., 2021), however, transcriptomics also allow for the possibility to identify differences in constitutive expression that could contribute to host resistance (Yuan et al., 2018).

Induced defences require pathogen/pest recognition either through microbe-/damage-associated molecular patterns (MAMPs/DAMPs), resulting in pattern triggered immunity (PTI), or effector recognition by host resistance (R) proteins, resulting in effector triggered immunity (ETI; Agrios, 2005; Dodds & Rathjen, 2010; Jones & Dangl, 2006; Spoel & Dong, 2012). The majority of plant R proteins consist of nucleotide-binding leucine rich repeat (NLR) receptors (Baggs et al., 2017; Głowacki et al., 2011). Multiple R genes have been described for the interaction between *P. taeda* and fusiform rust *Cronartium quercuum* f. sp *fusiforme* (Kubisiak et al., 2005; Quesada et al., 2014; Wilcox et al., 1996). These *P. taeda* R genes are allele-specific, conferring resistance only against rust isolates with the corresponding avirulence (Avr) effector gene (Wilcox et al., 1996). Conifer genomes have been shown to contain very large and diverse NLRs (Van Ghelder et al., 2019). Further expansion of these gene catalogues could aid studies aiming to map quantitative resistance traits for pine species.

Two major downstream defence response components in induced defence are modulation of secondary metabolite biosynthesis and pathogenesis-related (PR) gene expression. In conifers, stress responses include secretion of oleoresin, a complex mixture of terpenoids, phenolics (including flavonoids) and nitrogen compounds, as well as volatile emission (Keeling & Bohlmann, 2006; Maffei et al., 2011; Zulak & Bohlmann, 2010). Conifers have been shown to alter oleoresin composition and form traumatic resin ducts in xylem, where oleoresin accumulates, upon exposure to methyl jasmonate (MeJA; Zulak & Bohlmann, 2010). Many oleoresin components, including terpenoids and isoflavonoids, have direct antimicrobial activity (Maffei et al., 2011), thus modulation of these secondary metabolites, as well as constitutive differences between hosts, play an important role in host resistance.

This study expanded the transcriptomic resources available for tropical pine species and investigated both inducible and constitutive host defence mechanisms associated with resistance to *F. circinatum*. Transcriptomes were sequenced for three economically important tropical pines, *P. oocarpa*, *P. maximinoi* and *P. greggii*, in response to *F. circinatum* challenge using a comparable approach to previously sequenced transcriptomes for *P. tecunumanii* and *P. patula* (Visser et al., 2018). This enabled generation of a co-expression network to compare responses between multiple host species.

2 | MATERIALS AND METHODS

2.1 | Plant material

All plants were maintained in the Forestry and Agricultural Biotechnology Institute (FABI) *Fusarium* screening greenhouse at the University of Pretoria experimental unit for the duration of the trial. *P. oocarpa* (ca. 6 months old) and *P. greggii* var *australis* (ca. 4 months old) seedlings, from single open-pollinated families, were obtained from York Timbers (Sabie, South Africa). For *P. maximinoi* low germination rates precluded usage of seedlings, so rooted cuttings (ca. 6 months old) were obtained from SAFCOL (South African Forestry Company Limited).

2.2 | *F. circinatum* challenge

Plants were challenged with *F. circinatum* (isolate FCC3579, obtained from the FABI culture collection) as previously described (Visser et al., 2015). In short, apical buds of plants were mock-inoculated using 15% (v/v) sterile glycerol or inoculated with *F. circinatum* using spores suspended in 15% (v/v) sterile glycerol, adjusted to 5×10^4 spores/ml using a haemocytometer. Disease progression over time was tracked by measuring stem and lesion lengths weekly for 6 weeks post-inoculation to calculate the percentage live stem ([1 – lesion length/stem length]%). Decline in mean percentage live stem was compared between treatment groups over time for each host species using a Kruskal–Wallis rank sum test followed by a pairwise Wilcoxon rank sum test using Benjamini Hochberg (BH) multiple testing correction ($\alpha = 0.01$). The pathogen was re-isolated at 14 days post-inoculation (dpi) from diseased tissue on ½ strength potato dextrose agar (½ PDA; Merck). For each host species, tissue was harvested at 3- and 7-dpi for three biological replicates for each treatment group (inoculated and

mock-inoculated). Samples were flash frozen upon harvesting using liquid nitrogen and stored at −80°C. A single biological replicate consisted of the top 1 cm, from the inoculation point, of shoot tissue pooled from six seedlings.

2.3 | Data generation

Frozen tissue samples were sent to Novogene Corporation Inc. for total RNA isolation (proprietary method), library construction (strand specific with a 300 bp insert size) and sequencing (PE150) using the Illumina HiSeq. 2500 (Illumina). Data quality was assessed using FastQC (Andrews, 2010). Reference transcriptomes (*P. patula* = Pipt_v2.0, *P. tecunumanii* [LE] = Pnte_v1.0) and RNA-sequencing libraries for 3- and 7-dpi *F. circinatum* inoculated and mock-inoculated *P. patula* and *P. tecunumanii* (LE), from a previous study (Visser et al., 2018), were obtained from the National Centre for Biotechnology Information (NCBI) Transcriptome Shotgun Assembly (TSA) and Short Read Archive (SRA) databases.

2.4 | Combined de novo and genome-guided transcriptome assembly

Trimmomatic v0.36 (Bolger et al., 2014) was used to ensure read data contained no adapter sequences and to trim and filter sequences to ensure a minimum per base phred quality score of 30, reads shorter than 40 nt after trimming were discarded. Filtered read data was normalised in silico to a maximum coverage of 100X using Trinity v2.6.6 (Grabherr et al., 2011). Normalised reads were mapped to the *P. taeda* v2.01 genome assembly (https://treegenesdb.org/) using STAR v2.5.3a (Dobin et al., 2013). Trimmomatic filtered, normalised and mapped data sets were in turn assembled using Trinity to produce six preliminary transcriptomes per data set using *k*-mer values between 21 and 31 with a step of 2, giving a total of 12 de novo and six genome-guided Trinity assemblies (Supporting Information: Figure S1). A further 21 de novo assemblies were produced from the trimmomatic filtered data using transABySS v2.0.1 (Robertson et al., 2010) with *k*-mers ranging between 21 and 31 with a step of 2 as well as 33 and 89 with a step of 4. Minimum contig length was set to 350 for all assemblies. An assembly code was prefixed to sequence IDs for each preliminary assembly, to allow tracking of sequence origin (Supporting Information: Figure S1). Preliminary assemblies were subsequently concatenated and run through the EvidentialGene tr2aacds v2017.12.21 (Gilbert, 2013) pipeline to reduce redundancy and select for the optimal assembled transcript for each gene based on coding potential. Assembly metrics were calculated using transrate v1.0.3 (Smith-Unna et al., 2016).

The eukaryotic non-model transcriptome annotation pipeline v0.8.2 (EnTAP; Hart et al., 2019) was used to annotate primary transcripts resulting from EvidentialGene. GeneMarkS-T v5.1 March 2014 (Tang et al., 2015) was used to predict coding regions and resulting protein sequences. Similarity search alignments were performed using diamond v0.8.31 (Buchfink et al., 2014) against the *Arabidopsis thaliana* (TAIR10 release 2018.03), RefSeq (release 87), SwissProt (release 2018-03) and NCBI nonredundant (release 2018-03) protein databases with a minimum query coverage of 80% and minimum target coverage of 60%. EggNOG v0.12.7 (Huerta-Cepas et al., 2016) was used for further functional annotation. All non-pine origin sequences and unannotated contigs were discarded to produce the final transcriptomes for *P. oocarpa* (Pioo_v1.0), *P. greggii* (Pigr_v1.0) and *P. maximinoi* (Pima_v1.0). Remaining protein sequences were additionally annotated using Mercator (Lohse et al., 2014) to allow visualisation of expression in MapMan v3.5.1R2 (Thimm et al., 2014), as well as GhostKOALA (Kanehisa et al., 2016) to predict Kyoto Encyclopaedia of Genes and Genomes (KEGG) orthology (KO) of proteins. Benchmarking Universal Single Copy Orthologs (BUSCO) v3.0.2 (Simão et al., 2015; Waterhouse et al., 2017), with the eukaryote (n = 255), viridiplantae (n = 425) and embryophyte (n = 1,614) OrthoDB 10 databases, was used to determine the completeness and contiguity of assemblies.

2.5 | Gene family identification

Orthofinder 2.4.0 (Emms & Kelly, 2015) was used to cluster the three assembled proteomes with 120 other proteomes retrieved from the PLAZA (Van Bel et al., 2017; https://bioinformatics.psb.ugent.be/plaza/), TSA (https://www.ncbi.nlm.nih.gov/genbank/tsa/) and treegenes (Falk et al., 2018; Wegrzyn et al., 2019; https://treegenesdb.org/) databases (Supporting Information: Table S1), using default settings as in previous studies (Blande et al., 2017; Hill et al., 2016; Visser et al., 2018). A total of 4,280,273 protein sequences were clustered to identify putative gene families. The data included the proteomes of two red algae (*Cyanidioshyzon merolae* and *Chondrus cripus*) as outgroup, seven species of green algae, the liverwort *Marchantia polymorpha*, the moss *Physcomitrella patens*, the clubmoss *Selaginella moellendorffii*, three non-coniferous gymnosperms (*Cycas micholitzii*, *Ginkgo biloba*, *Gnetum montanum*), 21 coniferous gymnosperms (14 of which were *Pinus* spp.) and 87 angiosperms (Supporting Information: Table S1). Putative PR-gene orthogroups were identified using known PR-gene sequences (Custers et al., 2004; Fister et al., 2016; Marcus et al., 1997; Sooriyaarachchi et al., 2011) as previously described (Visser et al., 2018).

Putative NLR resistance (*R*) genes were identified by first extracting sequences associated with NB-ARC, TIR, RPW8, LRRNT and LRR1–LRR3 Pfam protein domains from eggNOG annotation. Domain organisation of these genes was characterised, as described Van Ghelder et al. (2019), using HMMER v3.3 (http://hmmer.org/) with the Pfam, TIGRFAM and superfamily HMM databases.

2.6 | Expression analysis

2.6.1 | Expression quantification

Kallisto v0.44.0 (Bray et al., 2016) was used to map reads to a combined host-pathogen reference transcriptome and quantify expression with 100 bootstrap samples and bias correction (Supporting Information: Figure S2). Kallisto output was imported into R v3.6.1 (R Core Team, 2019) with tximport v1.14.0 (Soneson et al., 2015). Transcripts with an average read count below 100 across at least three samples were filtered out as low-expression transcripts. For all mapping, the *P. tecunumanii* (Pnte_v1.0) transcriptome was used as host reference and the previously annotated *F. circinatum* transcriptome (Visser et al., 2019) obtained from the FSP34 genome assembly (B. D. Wingfield et al., 2012) was used as pathogen reference sequence and pathogen expression data was removed before host expression analysis.

2.6.2 | Differential expression

DESeq. 2 v1.26.0 (Love et al., 2014) was used to test for significant (Abs|Log_2(fold change)| ≥ 0.5, $p < 0.05$) differentially expressed genes (DEGs) in inoculated relative to mock-inoculated samples at each timepoint using a Wald test with Benjamini & Hochberg (BH) false discovery rate (FDR) correction.

2.6.3 | Co-expression network analysis

DESeq. 2 was used to normalise expression data and apply a variance stabilizing transformation. Batch effects between sequencing sets (*P. patula* and *P. tecunumanii* vs. *P. greggii* and *P. oocarpa*), were evaluated using principal component analysis (R Core Team, 2019) and removed using ComBat, from sva v3.34.0 (Leek et al., 2019). Variable stabilising transformed (VST) and batch corrected expression data for samples were clustered based on their Euclidean distance to identify outliers. Weighted Gene Co-expression Network Analysis (WGCNA) was performed to identify highly co-expressed genes using WGCNA v1.68 (Langfelder & Horvath, 2008, 2012). A signed-hybrid type of adjacency matrix was constructed with $\beta = 7$, the lowest soft-thresholding power for which the scale free topology fit was greater than 0.9 (Supporting Information: Figure S3), using biweight midcorrelation and transformed into a topological overlap matrix (TOM) to calculate dissimilarity. Average-linkage hierarchical clustering was used to cluster genes based on dissimilarity, co-expression modules identified using dynamic tree cut with a minimum module size of 30 and similar modules merged using a cut height of 0.25 (Supporting Information: Figure S4). The resulting network was visualised using Cytoscape v3.6 (Shannon et al., 2003). Module eigengenes (ME), a representation of expression for each module, were calculated and used to calculate correlation between modules and design factors. Additionally, gene significance (GS), which represents correlation between genes and samples, was calculated for each gene in each module.

2.6.4 | Enrichment analysis

Overrepresented gene ontology (GO) terms were identified using goseq v1.38.0 (Young et al., 2010) to test for significant enrichment (BH FDR, $p < 0.1$) of GO terms relative to the Pnte_v1.0 reference transcriptome annotation. GO enrichment was determined separately for up- and downregulated DEGs. GO-Figure (Reijnders & Waterhouse, 2021) was used to visualise enriched GO terms based on semantic similarity.

3 | RESULTS

3.1 | Relative host resistance to *F. circinatum*

Six-month-old seedlings of *P. greggii* (susceptible) and *P. oocarpa* (resistant) as well as rooted cuttings of *P. maximinoi* (moderately resistant), were inoculated with *F. circinatum* or mock-inoculated with sterile glycerol. Discoloration of stem and needles at the inoculation site was visible on all inoculated plants by 14-days post inoculation (dpi). Lesion development was more pronounced on *P. greggii* and *P. oocarpa* seedlings compared to the *P. maximinoi* cuttings (Supporting Information: Figure S5).

Disease progression was monitored by observing the decline in mean percentage live stem over 6 weeks (Figure 1). A marked decline in mean percentage live stem was observed for inoculated *P. greggii* seedlings over time, with significant differences (Wilcoxon rank sum test, $p < 0.01$) between inoculated and mock-inoculated groups already visible at 14 dpi, similar to *P. patula*. Disease progression in *P. maximinoi* cuttings and *P. oocarpa* seedlings peaked at ca. 21–28 dpi, with most inoculated plants showing signs of recovery by 42 dpi, similar to *P. tecunumanii*. The resistance observed for the *P. maximinoi* cuttings was higher than expected from previous trials using seedlings (Hodge & Dvorak, 2000, 2007). Consequently, while this species was retained for resource generation, it was excluded from expression analysis.

3.2 | Transcriptome assemblies

Shoot tissue was harvested from inoculated and mock-inoculated plants at 3- and 7-dpi for three biological replicates per group. RNA sequencing yielded between 29 and 40 million read pairs, representing between 9 and 12 Gb of sequence, per sample, resulting in a total of ca. 400 million read pairs per species representing ca. 120 Gb of

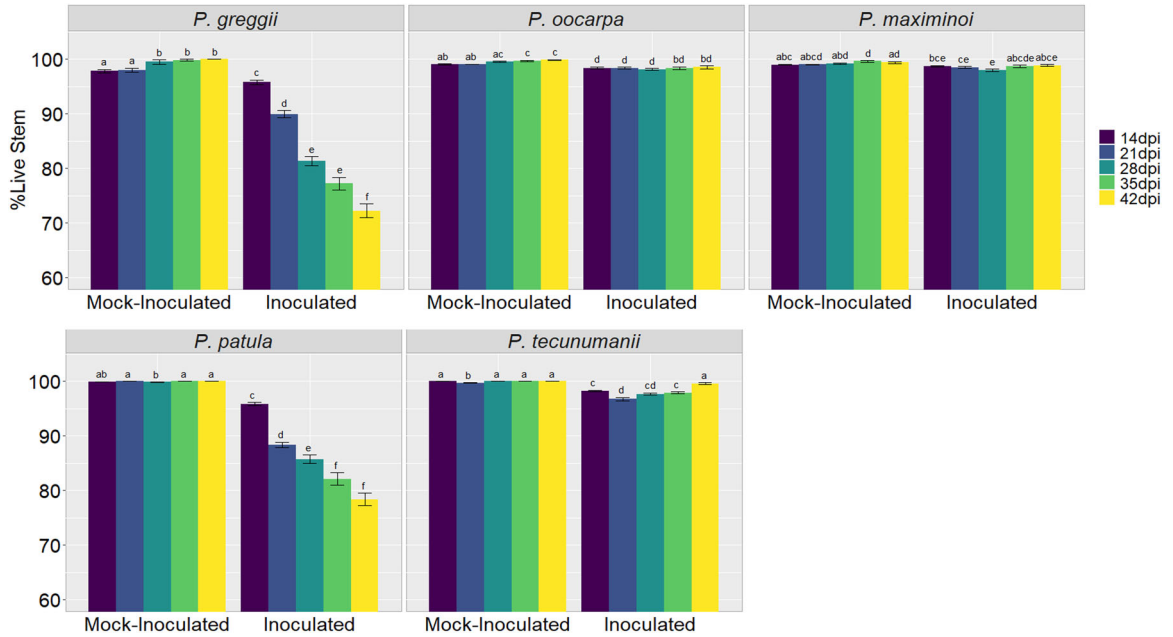

FIGURE 1 Disease progression over time on inoculated and mock-inoculated plants. Top: disease progression for *Pinus greggii*, *Pinus oocapra* and *Pinus maximinoi*. Bottom: previously observed disease progression for *Pinus patula* and *Pinus tecunumanii* (Visser et al., 2018). The *y*-axis represents the mean percentage live stem, with error bars representing standard error of the mean ($n = 20$). The *x*-axis represents inoculated and mock-inoculated groups between 14- and 42-days post-inoculation (dpi). For each host species, shared letters above bars indicate no significant difference between groups (Wilcoxon rank sum test, $p < 0.01$).

sequence (Supporting Information: Table S2). Read trimming and filtering with Trimmomatic reduced this to ca. 320 million reads (ca. 98 Gb) per species.

Preliminary transcriptome assembly using Trinity and Trans-ABySS produced 39 assemblies per species (Supporting Information: Figure S6). The EvidentialGenes pipeline was used to reduce redundancy across preliminary assemblies, resulting in ca. 92,000–149,000 transcripts (Supporting Information: Table S3). Functional annotation with EnTAP produced descriptions for >76% of sequences, of which ca. 50% were discarded as non-pine origin for each assembly, producing final assemblies consisting of 36,698 (Pigr_v1.0), 44,862 (Pnma_v1.0) and 32,285 (Pioo_v1.0) unigenes for *P. greggii*, *P. maximinoi* and *P. oocarpa*, respectively (Supporting Information: Data S1–S3). More than 70% of reads mapped back to each of the final assemblies (Supporting Information: Table S4). Similar to previous conifer assemblies, the top molecular function (MF) GO terms identified were nucleic acid binding terms (organic cyclic- and heterocyclic compound binding), hydrolase activity, transferase activity and ion binding (Figure 2), while the top biological process (BP) GO terms were indicative of growth, extensive metabolic activity and responses to stress, similar to previously assembled stress transcriptomes (Carrasco et al., 2017; Dunwell et al., 2008; Hernandez-Escribano et al., 2020; Visser et al., 2018; Wegrzyn et al., 2014).

The Benchmarking Universal Single Copy Ortholog (BUSCO) tool was used to assess assembly completeness. The *P. greggii*, *P. maximinoi* and *P. oocarpa* assemblies showed high completeness (>95%) and contiguity (>98%) with low redundancy (<6%) when compared against the Viridiplantae and Embryophyta BUSCOs (Supporting Information: Figure S7, Table S5). Completeness (>98%) and contiguity (>97%) was also high compared to the Eukaryota BUSCOs (Supporting Information: Figure S7, Table S5), though this lineage also showed more duplication (<27%). These quality metrics were similar to previously assembled high-quality gymnosperm transcriptomes (Supporting Information: Figure S7, Table S5).

3.3 | Comparison of gene families

OrthoFinder (Emms & Kelly, 2015) produced 100,173 orthogroups, containing 4005 506 (93.6%) proteins, of which 324 contained sequences from all 123 species. For the three assembled transcriptomes, ca. 97%–99% of predicted proteins were assigned to orthogroups, with ca. 0.02%–0.14% of proteins assigned to species-specific orthogroups (Supporting Information: Table S1).

3.3.1 | Identification of putative resistance genes

As nucleotide-binding, leucine-rich repeat (NLR) family proteins represent the main group of plant resistance (R) proteins, the full complement of assembled NLRs were identified for *P. greggii*, *P. patula*, *P. maximinoi*, *P. oocarpa* and *P. tecunumanii* LE. As described by Van Ghelder et al. (2019), protein sequences containing at least one of the canonical NB-ARC, resistance to powdery mildew 8 (RPW8) or Toll-interleukin 1 receptor (TIR) Pfam domains were considered NLRs

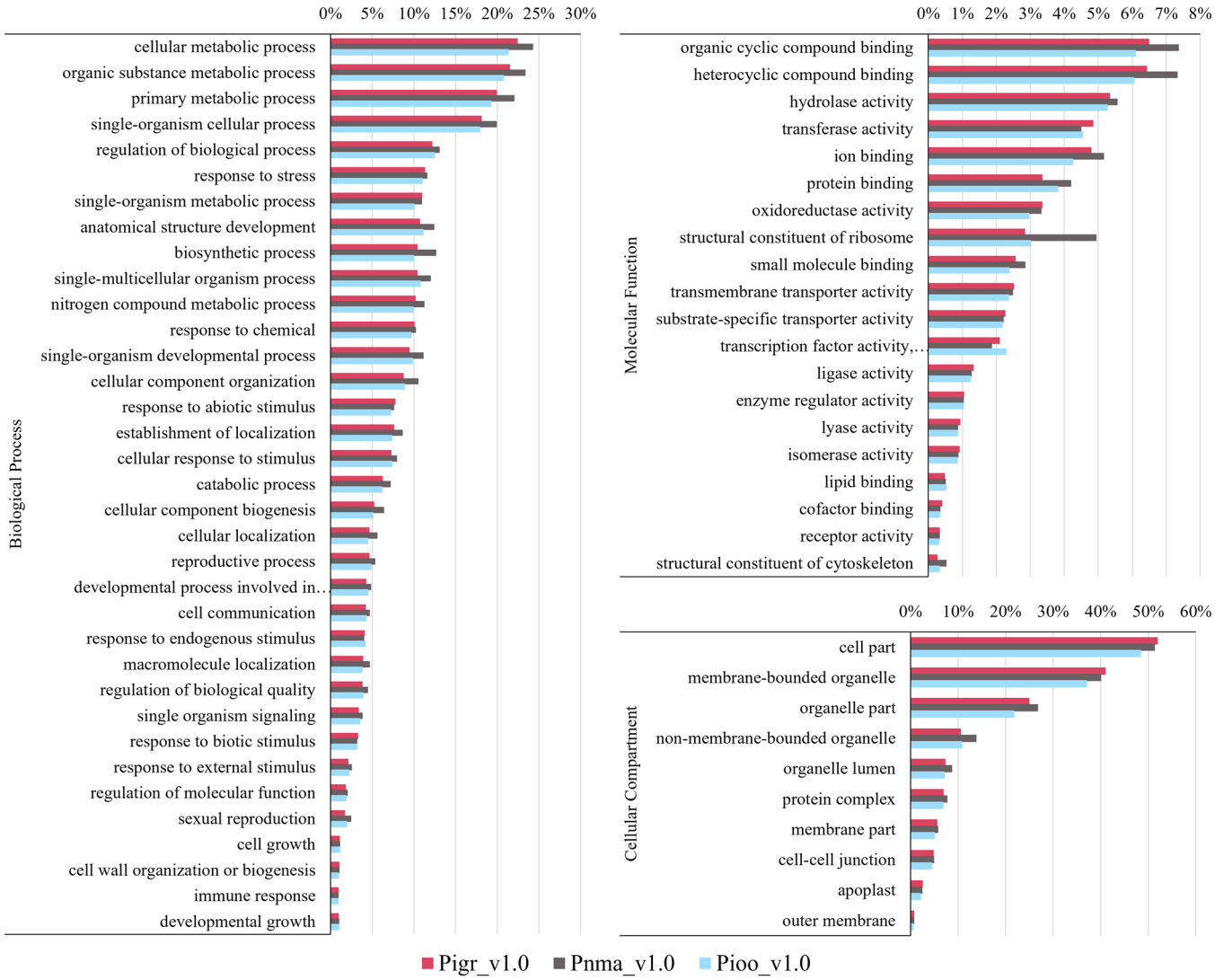

FIGURE 2 Distribution of biological process, molecular function and cellular compartment Gene Ontology (GO) terms in the assembled transcriptomes. Red—*Pinus greggii* v1.0 assembly. Grey—*Pinus maximinoi* v1.0 assembly. Blue—*Pinus oocarpa* v1.0 assembly. [Color figure can be viewed at wileyonlinelibrary.com]

TABLE 1 Nucleotide-binding leucine rich repeat (NLR) distribution across five pine transcriptomes

	Total NLRs	%NLR genes	TNL	CNL	RNL
Pinus greggii	382	1.02	196	145	41
Pinus patula	713	1.35	300	367	46
Pinus maximinoi	485	1.06	264	173	48
Pinus oocarpa	485	1.48	242	197	46
Pinus tecunumanii	676	2.36	262	361	53

while those containing only coiled-coil (CC) or leucine-rich repeat (LRR) domains were excluded as these domains are not NLR specific. The number of identified NLR genes ranged from 382 in *P. greggii* to 713 in *P. patula*, representing between 1.0% and 2.36% of the total assembled gene space (Table 1, Supporting Information: Table S6). Identified NLR genes were classified as TNL if a TIR domain was present, RNL if an RPW8 domain was present and CNL if neither of those domains were present.

3.3.2 | PR gene identification

Putative PR orthogroups were identified as previously described (Fister et al., 2016; Visser et al., 2018), using known PR-gene sequences from *A. thaliana*, *B. distachyon*, *P. trichocarpa* and *V. vinifera* for PR-1 through PR-17 (Fister et al., 2016), from *Helianthus annuus* and *Lactuca sativa* for PR-18 (Custers et al., 2004), and from *Macadamia integrifolia* and *P. sylvestris* for PR-19 (Asiegbu et al., 2003; Marcus et al., 1997). Due to the high homology between PR-15 and PR-16 families, and the expectation that PR-15 is monocot specific (Dunwell et al., 2008), no distinction was made between these

families and all putative PR-15 and PR-16 families were grouped as PR-16. Putative PR gene family orthogroups containing sequences from all conifer proteomes used were identified for 14 PR classes: PR-1, -2, -3, -4, -5, -7, -8, -9, -10, -11, -14, -16, -17, -18 (Supporting Information: Table S7).

The majority of conifer proteomes, including the assembled *P. maximinoi* and *P. oocarpa* proteomes, contained between one and three putative PR-6 members, however, as in previous studies, angiosperms on average had more putative PR-6 members (Supporting Information: Table S7). A single putative PR-12 defensin was identified from the *P. maximinoi* proteome, while the *P. greggii* and *P. oocarpa* assemblies each contained a putative PR-13 thionin. Aside from these three conifer genes, PR-12 was only represented by basal angiosperms and dicots, while PR-13 was only present in monocots and brassicaceae, as expected from previous studies.

Putative PR-19 members were identified for all conifer proteomes used excluding *Abies alba*, *P. cembra* and *P. lambertiana*. The absence of PR-19 members for these species is likely due to incomplete annotation rather than absence from the genomes. As in previous studies, while the putative PR-19 orthogroup contained sequences from *S. moellendorffii* as well as some basal angiosperms and a few monocots, PR-19 members were absent from the non-coniferous gymnosperms (Manners, 2009; Visser et al., 2018). Interestingly, although the PR-19 type sequence was originally identified from the dicot *M. integrifolia*, no dicot PR-19 members were identified, including from *M. integrifolia*. The only BLASTp hit in the *M. integrifolia* proteome (Maca016912-RA) for the type sequence MiAMP1 (P80915.1) was more than 400 amino acids longer and the alignment only covered 32% of the type sequence, suggesting that either the MiAMP gene is absent from the current assembly or the peptide is produced through cleavage of a precursor, though these antimicrobial peptides require further investigation in dicots.

3.4 | Constitutive differences associated with resistance

Filtering of low-expression transcripts resulted in 16 240 expressed genes across *P. greggii*, *P. patula*, *P. oocarpa* and *P. tecunumanii* seedlings. *P. maximinoi* was excluded from comparative expression analyses due to the unexpected response phenotype suggesting possible ontogenetic differences between seedlings and cuttings. A 7-dpi inoculated *P. tecunumanii* sample (Pt7IBR3) was identified as an outlier and discarded for network analysis (Supporting Information: Figure S8). Principal component analysis showed that ca. 37% of the variation within the data was associated with the separate sequencing batches (Supporting Information: Figure S9a), with principal component (PC) 1 separating *P. tecunumanii* and *P. patula* from *P. oocarpa* and *P. greggii*, while PC2 seemed to separate samples by host resistance. Following batch effect correction samples no longer showed separation based on sequencing batch (Supporting Information: Figure S9b), the new PC1 accounted for ca. 17% of the variation in the data and separated samples based on host resistance and treatment, while PC2 accounted for ca. 14% of variation and separated samples partially on harvesting timepoint.

A weighted gene co-expression network analysis (WGCNA) identified clusters of co-expressed genes in resistant and susceptible hosts. In total, WGCNA identified 43 co-expression modules, containing between 31 and 2,397 genes (Supporting Information: Table S8). Modules were numbered based on size, from largest to smallest. Module-trait correlations were calculated using module eigengenes (MEs) for each identified module with various levels of the trial design factors; treatment (inoculated/mock-inoculated), timepoint (3-/7-dpi), phenotype (resistant/susceptible hosts), as well as each host species (Supporting Information: Table S8).

Module M07 ($n = 705$, $r = 0.58$, $p = 6e\text{-}04$) had the highest correlation to treatment and 84.6% (597) of genes in this module were DEGs (Supporting Information: Tables S8 and S9). Module eigengene expression showed on average higher expression in all inoculated relative to mock-inoculated samples at both timepoints for resistant host species, while only 7-dpi inoculated *P. patula* samples showed higher expression of these genes for susceptible host samples (Supporting Information: Figure S10). This module was enriched for GO terms associated with pathogen recognition, mitogen activated protein kinase (MAPK) signalling, ET biosynthesis, phytohormone signalling responses to ET, JA and SA, increased transcription and translation, as well as terpenoid biosynthesis (Figure 3a, Supporting Information: Table S10).

Module M15 ($n = 467$, $r = 0.64$, $p = 8e\text{-}05$) had the highest positive correlation to harvesting timepoint (Supporting Information: Table S8), while M19 ($n = 294$, $r = -0.63$, $p = 1e\text{-}04$), M26 ($n = 164$, $r = -0.63$, $p = 1e\text{-}04$) and M29 ($n = 110$, $r = -0.82$, $p = 9e\text{-}10$) had the highest negative correlations to time. The M26 and M29 modules had no enriched GO terms. Genes in the M15 module mostly showed higher expression at 7- relative to 3-dpi in all samples, except some inoculated samples from resistant hosts (Supporting Information: Figure S11). Enriched GO terms for this module were mostly associated with cellular proliferation and growth (Figure 3b, Supporting Information: Table S10). The M19 module was enriched for GO terms associated with flavonoid biosynthesis, auxin transport and systemic responses to ET/JA signalling (Figure 3c, Supporting Information: Table S10). Genes in this module showed higher average expression at 3-dpi compared to 7-dpi in all hosts except *P. patula*, which showed low expression at both timepoints (Supporting Information: Figure S12). Interestingly, the decline on average expression of genes in this module was more pronounced in susceptible hosts.

The highest positive correlations to resistance phenotype (Supporting Information: Table S8) were M06 ($n = 731$, $r = 0.67$, $p = 3e\text{-}05$) and M02 ($n = 1\ 303$, $r = 0.92$, $p = 1e\text{-}16$). The M02 module showed higher module eigengene expression on average for all samples in resistant compared to susceptible hosts (Supporting Information: Figure S13). This module was enriched for MF and CC terms related to glutathione binding and the chloroplast (Supporting Information: Table S10), and contained numerous genes involved in the biosynthesis of phenylpropanoids, flavonoids, cysteine and

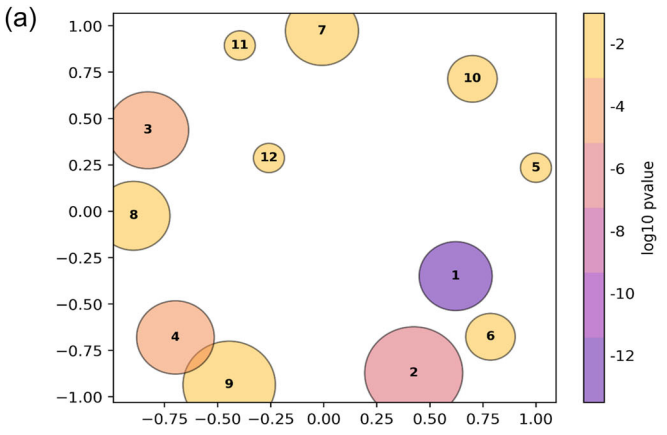

1. response to salicylic acid
2. response to jasmonic acid
3. translation
4. phosphorelay signal transduction sy...
5. immune response
6. response to salt stress
7. glucose catabolic process
8. ethylene biosynthetic process
9. positive regulation of RNA metaboli...
10. purine ribonucleotide transport
11. carbohydrate phosphorylation
12. isoprenoid biosynthetic process

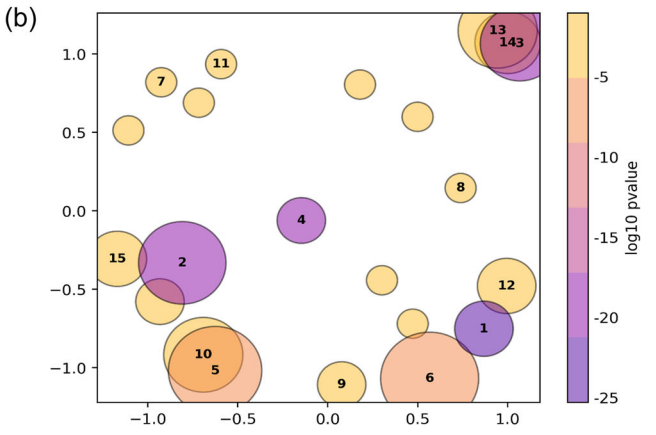

1. DNA replication
2. cytokinesis
3. regulation of mitotic cell cycle
4. cell cycle
5. DNA conformation change
6. DNA repair
7. stomatal complex development
8. regulation of gene expression by ge...
9. response to heat
10. chromatin organization
11. stomatal complex formation
12. organic substance biosynthetic proc...
13. regulation of cell cycle phase tran...
14. negative regulation of cell cycle p...
15. anastral spindle assembly involved ...

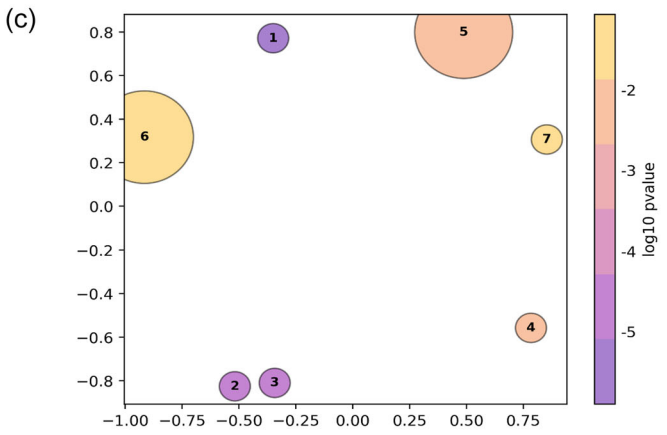

1. flavonoid metabolic process
2. proanthocyanidin biosynthetic proce...
3. phenol-containing compound biosynth...
4. regulation of flavonoid biosyntheti...
5. hypotonic salinity response
6. ion transport
7. response to jasmonic acid stimulus ...

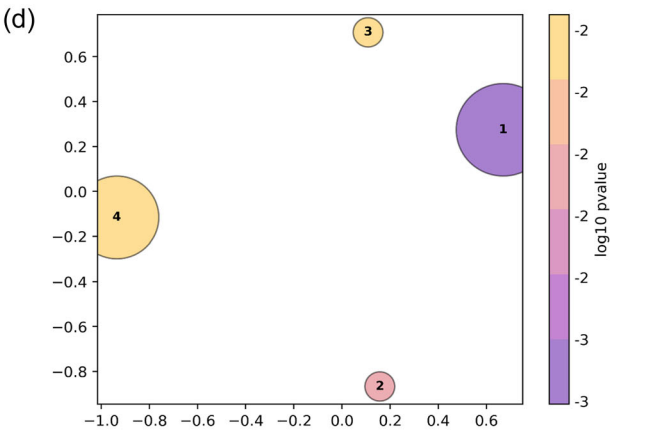

1. cellular response to starvation
2. protein tetramerization
3. cellular response to cold
4. positive regulation of cellular res...

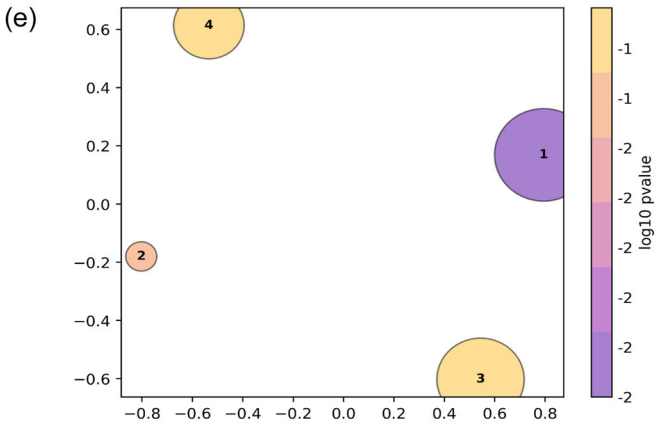

1. response to salicylic acid
2. cell septum edging catabolic proces...
3. innate immune response
4. carboxylic acid catabolic process

FIGURE 3 (See caption on next page)

methionine, as well as glutathione and sulfur metabolism. The M06 module also showed above-average eigengene expression for all *P. oocarpa* samples and below-average eigengene expression for all *P. greggii* samples (Supporting Information: Figure S14). While there was no clear pattern for most *P. patula* samples, 7-dpi inoculated samples also showed below-average eigengene expression. Additionally, although most *P. tecunumanii* samples showed higher than average eigengene expression, 7-dpi inoculated *P. tecunumanii* samples showed below-average eigengene expression for this module. This module was enriched for BP terms associated with responses to light intensity, seed and fruit development, and protein unfolding as well as CC terms associated with chloroplast and membrane bound organelles (Supporting Information: Table S10). Sulfur metabolism-related genes, *APS reductase*, *APS kinase*, *sulphite reductase*, two homologs of *serine acetyl transferase*, two homologs of *O-acetyl(thiol) lyase*, *glutathione synthetase*, and *cystathionine β lyase* were present within the M02 and M06 modules, and showed higher average expression in samples from resistant compared to susceptible hosts (Figure 4, Supporting Information: Table S11).

The highest negative correlations to resistance phenotype were M08 ($n = 697$, $r = -0.73$, $p = 7e\text{-}07$), M11 ($n = 582$, $r = -0.63$, $p = 1e\text{-}04$), M33 ($n = 69$, $r = -0.69$, $p = 1e\text{-}05$) and M04 ($n = 823$, $r = -0.95$, $p = 6e\text{-}22$). The M04 module had no enriched GO terms but contained many gibberellic acid (GA) biosynthesis genes, suggesting involvement of the GA signalling pathway in this module (Supporting Information: Table S12). Average eigengene expression for this module was higher in all susceptible relative to resistant samples (Supporting Information: Figure S15). Genes in the M08 module were enriched for GO terms related to responses to oxidative stress, cytoplasmic translation and NADPH regeneration. This module showed higher average eigengene expression in all *P. patula* samples, and lower average eigengene expression in *P. tecunumanii* samples, with about average eigengene expression for *P. greggii* and *P. oocarpa* samples (Supporting Information: Figure S16). The M33 module showed higher average eigengene expression in susceptible samples, excluding 7-dpi *P. patula* samples, relative to resistant samples (Supporting Information: Figure S17). This module was enriched for GO terms related to starvation and cold stress (Figure 3d). The M11 module was enriched for responses to SA and ET as well as various PTI-related BP terms (Figure 3e). Genes in this module showed higher expression in susceptible samples and lower expression in resistant samples (Supporting Information: Figure S18) similar to the M33 module (Supporting Information: Figure S17). Interestingly, this module also had a weak positive correlation with treatment ($r = 0.43$, $p = 2e\text{-}02$) as most inoculated resistant, but not susceptible, samples had higher eigengene expression for this module compared to mock-inoculated samples, suggesting that genes in this module could be *F. circinatum* responsive in resistant hosts.

3.5 | Host response comparison

Differential expression (DE) analysis, in inoculated relative to mock-inoculated samples, was performed to identify host response mechanisms underlying resistance and susceptibility to *F. circinatum* challenge at 3- and 7-dpi in *P. greggii* (susceptible) and *P. oocarpa* (resistant, Supporting Information: Table S9). This analysis was also repeated for *P. patula* (susceptible) and *P. tecunumanii* (resistant) data previously analysed (Visser et al., 2019) to allow for comparison between hosts with similar resistance phenotypes to *F. circinatum* challenge.

DE analysis for *P. greggii* identified 208 differentially expressed genes (DEGs) at 3-dpi and 43 DEGs at 7-dpi (Figure 5, Supporting Information: Table S9). In *P. oocarpa*, DE analysis identified 269 DEGs at 3-dpi and 603 DEGs at 7-dpi. Interestingly, while more DEGs were identified at the later timepoint compared to the earlier timepoint for *P. oocarpa*, similar to previous studies (Carrasco et al., 2017; Hernandez-Escribano et al., 2020; Visser et al., 2019), *P. greggii* showed a decrease in the number of DEGs over time (Figure 5).

3.5.1 | Responses underlying susceptibility

Upregulated DEGs at 3-dpi in *P. greggii* included: five putative *PR-16* genes (the only PR genes upregulated by *P. greggii*, Table 2, Supporting Information: Table S9), a single putative *R*-gene (Table 3, Supporting Information: Table S9), two *auxin-induced protein* genes, the first three genes involved in jasmonic acid (JA) biosynthesis (*LOX*, *AOS* and *AOC*, Figure 6, Supporting Information: Table S9), two genes involved in flavonoid and anthocyanin biosynthesis (*DFR*, *anthocyanidin reductase*), a single gene involved in abscisic acid biosynthesis (*carotenoid cleavage dioxygenase*), and a *methyl esterase 1* gene (Supporting Information: Table S9). No gene ontology (GO) terms were enriched for upregulated genes at 3-dpi.

Downregulated genes at 3-dpi had 24 enriched cellular compartment GO terms (Supporting Information: Table S13), mostly related to cytosolic translation, as well as cell-cell junctions, plasmodesma and the symplast. Of the downregulated DEGs, 21 coded for

FIGURE 3 Semantic similarity scatterplots summarising enriched biological process GO terms for modules significantly correlated with trial design factors. (a) Module M07 ($n = 705$) showed positive correlation with treatment ($r = 0.58$, $p = 6e\text{-}04$). (b) Module M15 ($n = 467$) showed positive correlation to timepoint ($r = 0.64$, $p = 8e\text{-}05$). (c) Module M19 ($n = 294$) showed negative correlation to timepoint ($r = -0.63$, $p = 1e\text{-}04$). (d) Module M33 ($n = 69$) showed negative correlation to phenotype ($r = -0.69$, $p = 1e\text{-}05$). (e) Module M11 ($n = 582$) showed negative correlation to phenotype ($r = -0.63$, $p = 1e\text{-}04$), as well as weak positive correlation to treatment ($r = 0.43$, $p = 2e\text{-}02$). Axes represent semantic space X and Y, circles represent GO terms arranged by similarity within the semantic space. Circle size is scaled by the number of enriched GO terms represented and circles are coloured based on the goseq $\log_{10}$(FDR) for enriched terms.

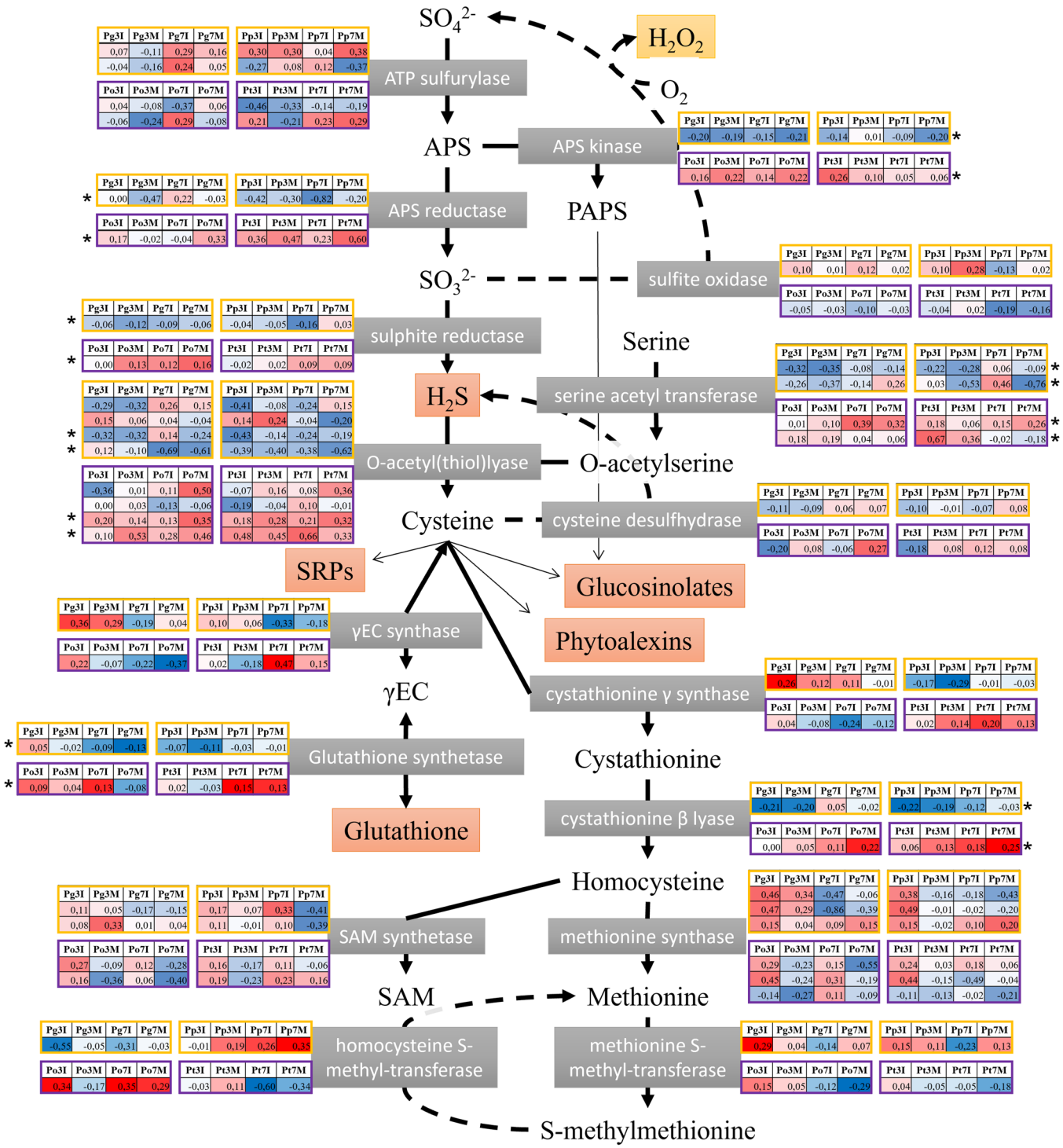

FIGURE 4 Summary of sulfur metabolism related gene expression within the co-expression network. Expression values represent average (across three biological replicates) VST expression relative to the mean for each gene at both timepoints (3- and 7-days post inoculation) in inoculated (I) and mock-inoculated (M) samples for each host (Pg, *Pinus greggii*; Pp, *Pinus patula*; Po, *Pinus oocarpa*; Pt, *Pinus tecunumanii*). Tables are outlined to indicate susceptible (orange) and resistant (purple) hosts. *Represents genes within the M02 and M06 modules, with positive correlations to host resistance phenotype. Expression tables are grouped by host response phenotype, with susceptible hosts (*P. greggii* and *P. patula*) on top and resistant hosts (*P. oocarpa* and *P. tecunumanii*) on the bottom, and rows correspond to putative homologs within the co-expression network. Thick black lines represent direct enzymatic steps, thin black lines represent multi-step processes leading to downstream production, dashed grey lines show points in the pathway where product can be reconverted into substrate. Grey boxes represent enzymes, the yellow box highlights peroxide which could act as a defence signal, orange boxes represent products of sulfur metabolism that have been associated with roles in defence, so-called sulfur defence compounds. APS, adenosine 5′-phosphosulfate; PAPS, 3′-phosphoadenosine 5′-phosphosulfate; SAM, S-adenosyl methionine; SRP, sulfur-rich proteins.

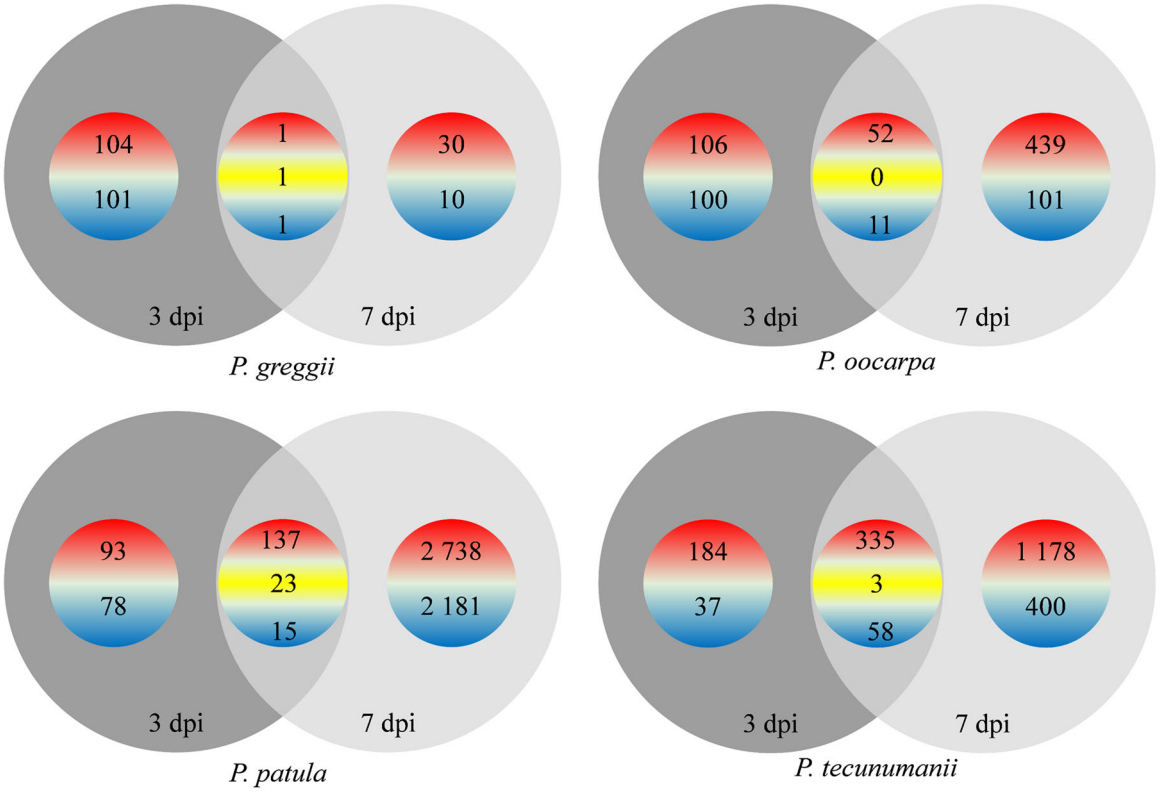

FIGURE 5 Comparison of differentially expressed genes in inoculated relative to mock-inoculated samples in *Fusarium circinatum* susceptible and resistant pines between timepoints. Numbers in red represent upregulated genes, numbers in blue represent downregulated genes, numbers in yellow represent contra-regulated genes (genes upregulated at one timepoint and downregulated at the other. dpi, days postinoculation. Data for *Pinus patula* and *Pinus tecunumani* originate from a previous study (Visser et al., 2018).

ribosomal proteins and 10 were involved in RNA recognition, binding and processing (Supporting Information: Table S9). Additionally, a *UGT73B5*, a flavonol 3-O-glucosyltransferase putatively associated with anthocyanin and flavonol glycoside biosynthesis from flavonoids, as well as an *isoflavone reductase gene* were also downregulated.

The few upregulated DEGs at 7-dpi included a *cytokinin oxidase* gene, a *LOX* gene (Figure 6), an *ABA stress ripening* (*ASR*) gene and three ABA receptor genes, resulting in enrichment for the molecular function term abscisic acid binding (Supporting Information: Table S13). The 7-dpi downregulated genes had no enriched GO terms, though included a *UGT73B5*, as well as a chitin recognition protein gene and two putative *R*-genes (Table 3, Supporting Information: Table S9), one of which was also downregulated in *P. patula* at 3-dpi and upregulated in *P. tecunumanii* at 7-dpi (Supporting Information: Table S9).

Only three DEGs were present at both timepoints (Figure 5). These were, a predicted *RING-H2 finger* gene upregulated at both timepoints, an uncharacterized protein gene downregulated at both timepoints and a *BEACH domain-containing* gene upregulated at 3-dpi and downregulated at 7-dpi (Supporting Information: Table S9).

Interestingly, of the 157 putative *R*-genes showing differential expression in at least one host (66 TNL, 71 CNL, 20 RNL), 127 (54 TNL, 56 CNL, 17 RNL) were only differentially expressed by *P. patula* at 7-dpi. Additionally, only 3 (2 TNL, 1 CNL) of these were upregulated (Supporting Information: Table S9).

3.5.2 | Responses in resistant hosts

Upregulated DEGs at 3-dpi in *P. oocarpa* were enriched for BP, MF and CC GO terms related to gene expression and cytosolic translation (Supporting Information: Table S14). The only phytohormone signalling-related DEGs were two *PAD4* genes, involved in salicylic acid (SA) signalling, a *12-oxophytodienoate reductase* (*OPR*) gene, involved in JA biosynthesis and induced by JA signalling (Figure 6), an *IAMT1*, involved in auxin methylation, and a *1-aminocyclopropane-1-carboxylase synthase* (*ACS*), a gene involved in ethylene (ET) biosynthesis that was upregulated at all timepoints in both resistant hosts (Figure 7, Supporting Information: Table S9). Upregulated genes at 3-dpi in *P. oocarpa* also included 11 putative *R*-genes, three of which were also upregulated at 7-dpi (Table 3, Supporting Information: Table S9), a putative *PR-1* which was also upregulated at 3-dpi in *P. tecunumanii*, a putative *PR-3* and *PR-5* which were upregulated at both timepoints in *P. oocarpa* as well as *P. tecunumanii*, and three putative *PR-9* genes, two of which were also upregulated at both timepoints in both resistant hosts (Table 2, Supporting Information: Table S9).

TABLE 2 Comparison of putative pathogenesis-related genes differentially expressed in *Pinus greggii* and *Pinus oocarpa* to *Pinus patula* and *Pinus tecunumanii*

	Susceptible hosts				Resistant hosts			
	P. greggii		*P. patula*		*P. oocarpa*		*P. tecunumanii*	
Gene	3-dpi	7-dpi	3-dpi	7-dpi	3-dpi	7-dpi	3-dpi	7-dpi
PR-1_04	-	-	−1.38	-	2.15	-	0.95	-
PR-1_14	-	-	-	2.63	-	3.05	-	1.83
PR-1_01	-	-	-	1.07	-	2.31	-	2.17
PR-2_02	-	-	-	2.03	-	2.85	1.14	1.42
PR-2_08	-	-	-	1.54	-	2.72	-	1.96
PR-3_02	-	-	-	1.87	2.00	3.98	1.55	1.98
PR-3_16	-	-	-	2.00	-	4.46	1.55	1.00
PR-3_09	-	-	-	1.53	-	1.82	-	2.28
PR-3_10	-	-	-	-	-	1.83	-	0.97
PR-3_13	-	−2.32	-	-	-	-	-	1.05
PR-3_08	-	-	-	0.60	-	−1.62	-	-
PR-3_06	-	-	-	0.73	-	−2.00	-	-
PR-4_01	-	-	-	1.93	-	3.40	1.53	1.46
PR-4_02	-	-	-	1.16	-	1.45	0.76	1.05
PR-4_03	-	-	-	1.76	-	1.64	-	2.03
PR-5_06	-	-	-	0.98	2.19	4.71	1.65	2.51
PR-5_07	-	-	-	1.05	-	3.23	1.19	1.58
PR-5_30	-	-	-	1.56	-	1.85	1.31	0.97
PR-5_25	-	-	-	1.12	-	1.14	0.96	-
PR-5_17	-	-	-	1.63	-	2.66	-	2.43
PR-5_01	-	-	-	1.75	-	1.75	-	1.83
PR-5_03	-	-	-	-	-	2.97	-	0.71
PR-5_38	-	-	-	1.68	-	3.25	-	-
PR-5_19	-	-	-	-	-	6.07	-	-
PR-5_27	-	-	-	-	-	2.15	-	-
PR-7_04	-	-	-	-	−0.95	-	-	-
PR-9_14	-	-	-	4.81	6.67	7.16	1.82	1.82
PR-9_27	-	-	-	1.86	3.46	4.75	1.25	1.62
PR-9_16	-	-	-	0.59	2.62	-	-	0.85
PR-9_33	-	-	-	1.77	-	3.08	1.14	1.29
PR-9_21	-	-	-	1.79	-	3.06	1.15	1.08
PR-9_36	-	-	-	2.19	-	3.68	-	1.61
PR-10_03	-	-	-	1.32	-	3.45	−0.73	0.76
PR-11_01	-	-	-	2.34	-	2.89	1.22	1.69
PR-16_06	-	-	-	1.34	2.70	3.80	1.65	-
PR-16_36	-	-	-	1.10	3.11	3.48	-	2.07
PR-16_10	-	-	-	-	0.94	-	1.00	-
PR-16_40	-	-	-	-	3.41	-	-	1.22

TABLE 2 (Continued)

	Susceptible hosts				Resistant hosts			
	P. greggii		*P. patula*		*P. oocarpa*		*P. tecunumanii*	
Gene	3-dpi	7-dpi	3-dpi	7-dpi	3-dpi	7-dpi	3-dpi	7-dpi
PR-16_35	-	-	-	-	7.13	-	-	-
PR-16_23	-	-	-	-	2.62	-	-	-
PR-16_31	-	-	-	−1.05	3.66	-	-	-
PR-16_27	-	-	-	−1.31	2.21	-	-	-
PR-16_48	-	-	−1.00	−1.19	1.96	-	-	-
PR-16_29	-	-	-	2.95	-	2.50	-	2.09
PR-16_38	-	-	-	1.94	-	1.25	-	1.27
PR-16_14	-	-	-	-	-	0.86	-	-
PR-16_58	-	-	-	−2.01	-	0.61	-	-
PR-16_18	0.79	-	-	-	-	-	-	-
PR-16_62	1.17	-	-	-	-	-	-	-
PR-16_20	1.75	-	-	-	-	-	-	-
PR-16_19	1.99	-	-	-	-	-	-	-
PR-16_52	1.01	-	-	−1.20	-	-	-	-
PR-17_02	-	-	-	2.13	-	2.41	-	1.27
PR-18_02	-	-	-	2.61	-	2.71	1.82	2.09
PR-19_01	-	-	-	0.66	-	1.67	-	0.65

Note: The gene list was limited to only PR genes differentially expressed in *P. greggii* and/or *P. oocarpa*. Values represent significant (FDR < 0.05) Log2 (Fold Change) in inoculated relative to mock-inoculated samples.

Downregulated DEGs at 3-dpi were enriched for BP and CC GO terms related to photosynthesis, RNA stabilization and plastid organisation (Supporting Information: Table S14). Downregulated DEGs also included a *UGT73B5* that was downregulated at both timepoints, an *ASR* gene, an auxin response factor, and an *auxin induced protein* gene that was also downregulated in *P. greggii* (Supporting Information: Table S9).

Upregulated DEGs at 7-dpi were enriched for BP GO terms related to responses to chitin, JA and ET as well as terpenoid biosynthesis (Supporting Information: Table S14). DEGs included nine putative *R*-genes, an *ACS* and an *ACO* gene, an *ETR1* as well as an *RTE1* gene, an *ET response factor* (*ERF*), a *PAD4*, an *OPR*, *LOX* genes, multiple *JAZ* and *auxin-induced* genes as well as a *GID1A* receptor gene (Figures 6, 7, Supporting Information: Table S9). Additionally, upregulated DEGs included multiple putative *PR*-genes, many of which were also upregulated in *P. tecunumanii* (Table 2, Supporting Information: Table S9).

Downregulated DEGs at 7-dpi were enriched for BP GO terms related to xylem and phloem formation and CC GO terms related to the chloroplast (Supporting Information: Table S14). Downregulated DEGs included two putative *PR-3* genes (Table 2, Supporting Information: Table S9) as well as two genes involved in JA biosynthesis (*AOS* and *OPCL*, Figure 6, Supporting Information: Table S9).

4 | DISCUSSION

Multiple studies have quantified *F. circinatum* resistance of *Pinus* spp. by measuring lesion development on seedlings (Hodge & Dvorak, 2000, 2007; Mitchell et al., 2012; Roux et al., 2007). These studies consistently showed high susceptibility to *F. circinatum* challenge for *P. patula* and *P. greggii* with relatively high resistance for *P. oocarpa* and low elevation *P. tecunumanii*. The contrasting resistance and susceptibility of low elevation *P. tecunumanii* and *P. patula* to *F. circinatum* challenge have previously been confirmed and used as a pathosystem to investigate the host-pathogen interaction between *Pinus* spp. and *F. circinatum* (Visser et al., 2018; Visser et al., 2019). Disease progression over time confirmed the expected *F. circinatum* resistance of *P. oocarpa* seedlings as well as the expected susceptibility of *P. greggii* seedlings, allowing expansion of the pathosystem to include two resistant and two susceptible *Pinus-F. circinatum* interactions for further molecular biology insights.

The three assembled transcriptomes add to the ever-growing index of conifer reference sequences, a valuable resource for conservation and forestry, and the orthogroups identified can also be used in future to identify and characterize other important gene families within tropical pines. Accordingly, the transcriptomes in this study formed part of the data set used to design the Pitro50K tropical pine SNP chip (Jackson et al., 2021). Additionally, in combination with

TABLE 3 Summary of putative resistance (*R*) genes differentially expressed in response to *Fusarium circinatum* challenge

		Susceptible hosts				Resistant hosts			
		P. greggii		*P. patula*		*P. oocarpa*		*P. tecunumanii*	
Gene	NLR-type	3-dpi	7-dpi	3-dpi	7-dpi	3-dpi	7-dpi	3-dpi	7-dpi
Pnte31HSn_TRINITY_DN77221_c1_g1	TNL	-	-	-	−1.69	0.60	-	-	-
Pnte31HS_TRINITY_DN112489_c0_g1	TNL	-	-	-	−1.44	-	1.49	-	-
Pnte31HSn_TRINITY_DN88838_c4_g2	TNL	-	-	-	−1.39	-	1.28	-	-
Pnte25LSn_TRINITY_DN99813_c1_g4	TNL	-	-	-	-	0.97	-	-	-
Pnte31HSn_TRINITY_DN85734_c0_g9	TNL	-	-	-	-	1.07	-	-	1.10
Pnte31LSn_TRINITY_DN100564_c13_g1	TNL	-	-	-	-	-	-	-	1.25
Pnte31LS_TRINITY_DN126865_c0_g2	TNL	-	−5.73	-	-	-	-	-	-
Pnte31LSn_TRINITY_DN99240_c0_g1	TNL	-	−6.15	-0.99	-	-	-	-	1.04
Pnte31LSn_TRINITY_DN100433_c3_g1	TNL	-	-	-	-	-	2.47	-	-
Pnte31HSn_TRINITY_DN85689_c0_g1	TNL	-	-	-	-	-	0.93	-	-
Pnte25LS_TRINITY_DN125236_c0_g8	TNL	-	-	-	-	-	-	-	0.85
Pnte25HSn_TRINITY_DN82026_c1_g2	TNL	-	-	-	0.83	-	0.84	-	-
Pnte31LSng_TRINITY_GG_11029_c10_g1	CNL	-	-	-	−2.95	1.78	-	-	-
Pnte31LS_TRINITY_DN127426_c12_g3	CNL	-	-	-	−1.36	1.31	1.09	-	-
Pnte25HSng_TRINITY_GG_52253_c1_g1	CNL	-	-	-0.67	−1.29	-	-	-	-
Pnte25LSn_TRINITY_DN100613_c3_g3	CNL	-	-	-	−0.97	0.95	-	-	-
Pnte31HS_TRINITY_DN113197_c8_g1	CNL	-	-	-	−0.97	0.68	-	-	-
Pnte31LSng_TRINITY_GG_43676_c1_g3	CNL	-	-	-	−0.96	-	-	-	0.81
Pnte25LSng_TRINITY_GG_79990_c0_g3	CNL	-	-	-	−0.86	1.12	-	-	-
Pnte25HSng_TRINITY_GG_39472_c0_g1	CNL	1.46	-	-	-	-	-	-	-
Pnte25LSng_TRINITY_GG_53595_c2_g1	CNL	-	-	-	-	0.80	0.86	-	-
Pnte31LSng_TRINITY_GG_61666_c0_g1	CNL	-	-	-	-	2.39	2.16	-	-
Pnte25HSn_TRINITY_DN88591_c2_g2	CNL	-	-	-	-	-	-	-	0.63
Pnte25LSn_TRINITY_DN100422_c0_g2	CNL	-	-	-	-	-	−2.73	-	-
Pnte31HS_TRINITY_DN113003_c7_g2	CNL	-	-	-	-	-	-	-	−0.70
Pnte31HSng_TRINITY_GG_54512_c8_g1	CNL	-	-	-	-	2.75	-	-	-
Pnte31HSng_TRINITY_GG_51897_c1_g2	CNL	-	-	−1.05	-	-	-	-	-
Pnte25HSng_TRINITY_GG_18986_c0_g1	RNL	-	-	-	−1.05	-	1.49	-	-
Pnte25HS_TRINITY_DN112081_c0_g2	RNL	-	-	-	-	-	-	0.96	-
Pnte25LS_TRINITY_DN119343_c3_g1	RNL	-	-	-	-	-	-	-	0.55

Note: *R*-genes differentially expressed only in *P. patula* at 7-dpi (days post inoculation) were excluded. Values represent significant (FDR < 0.05) Log2 (Fold Change) in inoculated relative to mock-inoculated samples.

previously assembled pine references, a repertoire of tropical pine sequences was identified for two important families of defence-related genes, NLR receptor genes and PR defence response genes. As expected from previous studies, the number of expressed putative NLR genes identified represented substantial proportions of the gene space relative to angiosperm transcriptomes (Van Ghelder et al., 2019). PR gene family members could be identified in all assembled transcriptomes for almost all the PR gene families known to be present in conifers except PR-6, which was absent from the *P. greggii*, *P. monticola* and *P. tecunumanii* proteomes. The low copy number of PR-6 genes identified in other conifer proteomes suggest the possibility that PR-6 might have been lost in these species, however, insufficient data is available at this time to determine whether the gene is missing only from the assemblies or the genome.

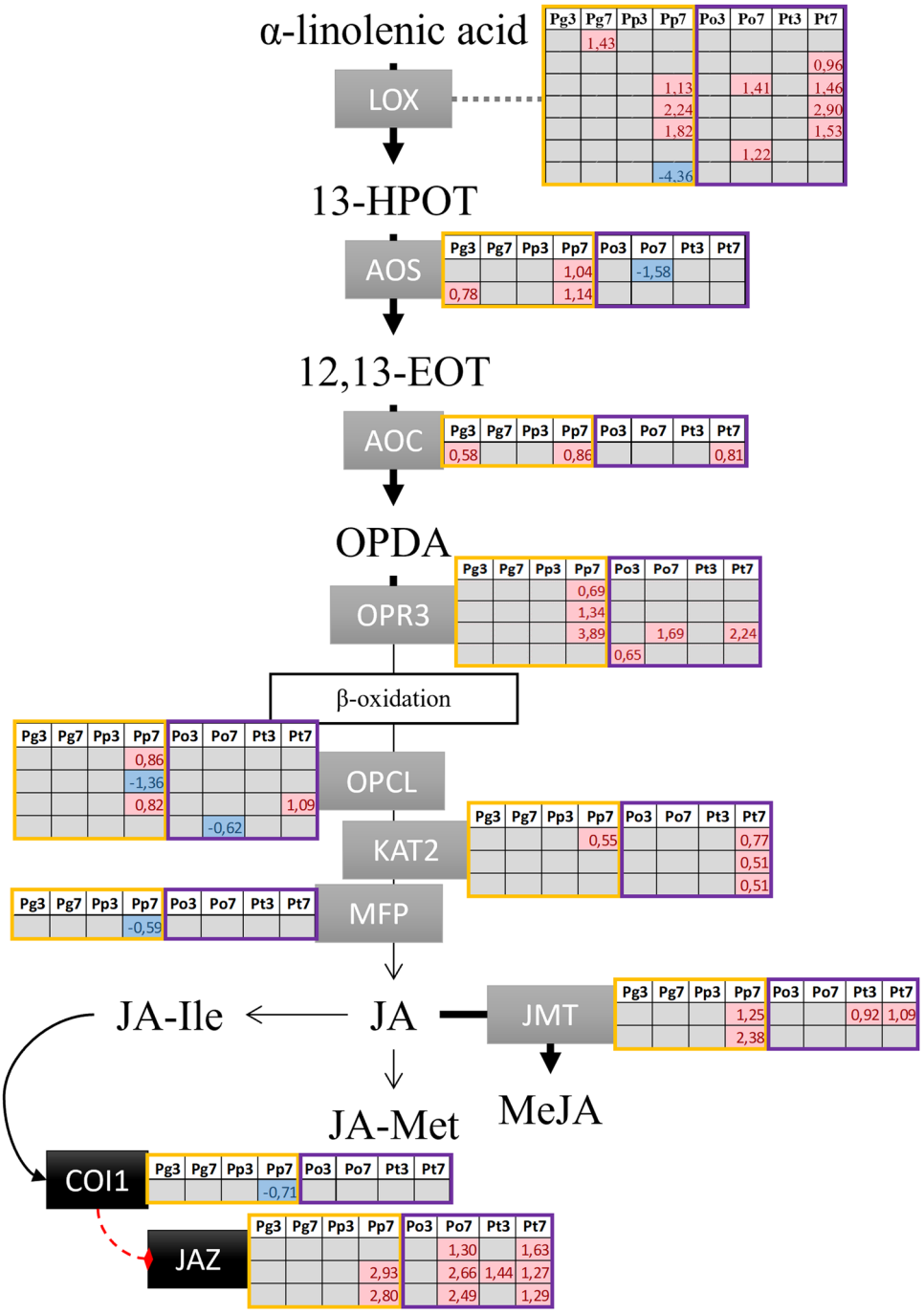

FIGURE 6 Summary of differentially expressed genes involved in jasmonic acid biosynthesis and signalling. Values in tables represent significant Log_2(Fold Change) in inoculated relative to mock-inoculated samples for each host species (Pg, *Pinus greggii*; Pp, *Pinus patula*; Po, *Pinus oocarpa*; Pt, *Pinus tecunumanii*) at 3- and 7-days postinoculation. Tables are outlined to indicate susceptible (orange) and resistant (purple) hosts. Rows in tables correspond to putative homologs. Grey boxes represent enzymes, Borderless text represents metabolic compounds. Black bordered text represents processes. Black boxes represent phytohormone receptor and signalling components. Thick black lines represent direct enzymatic steps. Thin black lines represent multistep processes or interaction between phytohormones and signalling components. Dashed red lines represent inhibition. 12,13-EOT, 12,13(S)-epoxy-octadecatrienoic acid; 13-HPOT, 13(S)-hydroperoxy-octadecatrienoic acid; AOC, allene oxide cyclase; AOS, allene oxide synthase; COI1, coronatine insensitive 1; JA, jasmonic acid; JA-Ile, jasmonoyl isoleucine; JAZ, jasmonate-zim-domain protein; JMT, jasmonate methyl transferase; KAT2, 3-ketoacyl-CoA thiolase; LOX, lipoxygenase; MeJA, methyl-jasmonate; MFP, multifunctional protein; OPCL, 3-oxo-2-(2'(Z)-pentenyl)-cyclopentane-1-octanoic acid ligase; OPDA, oxophytodienoic acid; OPR3, OPDA reductase 3.

4.1 | Induced responses show similarity between resistant hosts

P. oocarpa responses suggested active defence at 3-dpi that amplify and diversify over time to 7-dpi. Upregulation of multiple putative *R*- and *PR*-genes combined with downregulation of genes involved in photosynthesis at 3-dpi indicated active defence responses. While the low number of phytohormone-related *P. oocarpa* DEGs limited investigation of these pathways at 3-dpi, upregulation of biosynthesis genes suggested possible involvement of JA and ET signalling while upregulation of an *IAMT* and downregulation of an *ASR* as well as an *auxin induced protein* gene suggested suppression of auxin. Auxin is a central regulator of phytohormone signalling and has been shown to have antagonistic effects on JA signalling (Grunewald et al., 2009). Thus, suppression of auxin could allow for JA signalling. This differs from the 3-dpi responses previously observed for *P. tecunumanii*, which pointed to active auxin and ET signalling with suppressed JA signalling (Visser et al., 2019). This could suggest differences in timing of earlier defence responses between these resistant species, however, this requires further investigation as only a few DEGs were associated with these pathways. At 7-dpi for *P. oocarpa*, a larger complement of ET and JA biosynthesis and response genes were upregulated, suggesting amplified signalling by these pathways. Additionally, in contrast to 3-dpi, multiple auxin responsive genes were upregulated, suggesting involvement of auxin signalling at 7-dpi. Although no SA biosynthesis-related genes were differentially expressed by *P. oocarpa*, upregulation of *PAD4* genes suggest a role for SA signalling at both timepoints (Zhou et al., 1998). These responses are similar to the 7-dpi responses observed for *P. tecunumanii* (Visser et al., 2019).

The importance of both SA as well as JA and ET signalling pathways in host resistance to *F. circinatum* is further supported by module M07. Module eigengene expression was higher in inoculated samples from resistant hosts compared to susceptible and more than 80% of genes in this module were induced at some point in resistant hosts. Transcriptional responses in moderately resistant *P. pinaster* also indicated involvement of these three phytohormone signalling pathways (Hernandez-Escribano et al., 2020). Additionally, a comparison between resistant *Pinus pinea* and susceptible *P. radiata* challenged with *F. circinatum* observed upregulation of SA biosynthesis in the resistant host only, as well as more pronounced JA and ET responses in the resistant relative to the susceptible host (Zamora-Ballesteros et al., 2021).

Enriched GO terms for module M15 suggested increased expression of growth-related genes at 7- relative to 3-dpi in most samples, excluding inoculated samples from resistant hosts. Defence responses are metabolically expensive, often resulting in a trade-off between growth and defence (Huot et al., 2014). Thus, co-expression analysis suggested that resistant hosts activate defence responses earlier than susceptible hosts and suppress growth to allow for amplification of the responses over time, however, constitutive differences between hosts are also likely to contribute to resistance.

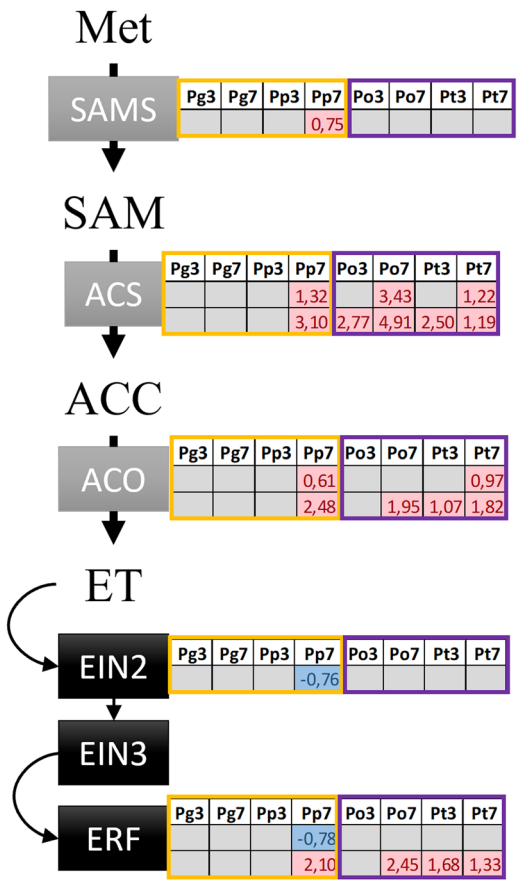

FIGURE 7 Summary of differentially expressed genes involved in ethylene biosynthesis and signalling. Values in tables represent significant Log_2(Fold Change) in inoculated relative to mock-inoculated samples for each host species (Pg, *Pinus greggii*; Pp, *Pinus patula*; Po, *Pinus oocarpa*; Pt, *Pinus tecunumanii*) at 3- and 7-days postinoculation. Tables are outlined to indicate susceptible (orange) and resistant (purple) hosts. Rows in tables correspond to putative homologs. Grey boxes represent enzymes, Borderless text represents metabolic compounds. Black bordered text represents processes. Black boxes represent phytohormone receptor and signalling components. Thick black lines represent direct enzymatic steps. Thin black lines represent interaction between phytohormones and signalling components. ACS, ACC-synthase; ACC 1-aminocyclopropane-1-carboxylic acid; ACO, ACC-oxidase; ET, ethylene; EIN, ethylene insensitive; ERF, ethylene response factor; Met, methionine; SAMS, SAM synthetase; SAM, S-adenosyl-l-methionine.

4.2 | Constitutive expression suggests a role for sulfur and flavonoid metabolism in resistance

Higher average eigengene expression, in resistant relative to susceptible hosts, of sulfur metabolism-related genes in modules M02 and M06 indicated the potential for rapid defence activation and higher constitutive levels of defence-related compounds. Plants capture sulfur by reducing inorganic sulphates to sulphides which are incorporated into cysteine allowing subsequent production of

important metabolites including methionine, biotin, glutathione and sulfur-containing defence compounds (Capaldi et al., 2015). Consequently, sulfur is associated with numerous metabolic pathways, including biotic stress, and sulfur deficiency has been associated with increased susceptibility of *Brassica napus* to *Leptosphaeria maculans*, *Botrytis cinerea* and *Phytophthora brassicae* (Dubuis et al., 2005). Thus, a higher constitutive capacity for sulfur assimilation and metabolism could allow for faster host responses.

Flavonoid biosynthesis could play important roles in host resistance to both pathogen challenge and wounding. Flavonoids are phenolic secondary metabolites involved in plant responses to biotic and abiotic stresses (Falcone Ferreyra et al., 2012; Truetter, 2006). GO enrichment of genes in module M02 suggest that resistant hosts have higher constitutive expression of flavonoid biosynthesis. Flavonoid phytoalexins have been shown to increase resistance to *Tobacco mosaic virus* in *Nicotiana tabacum* (Chong et al., 2002), *Phytophtora sojae* in *Glycine max* (Graham et al., 2007) and *Colletotrichum sublineolum* in *Sorghum bicolor* (Ibraheem et al., 2010). Additionally, flavonoid biosynthesis genes were upregulated in *P. pinea* but not *P. radiata* in response to *F. circinatum* challenge at 4-dpi (Zamora-Ballesteros et al., 2021). Thus, the higher constitutive expression of flavonoid biosynthesis-related genes in resistant relative to susceptible hosts observed in module M02 could contribute to resistance, suggesting that investigation of flavonoids in resistant hosts could yield phytoalexins targeting *F. circinatum*. Furthermore, both wounding and MeJA signalling have been shown to induce flavonoid biosynthesis in spruce (Richard et al., 2000). This points to the possibility that the decrease in expression of flavonoid biosynthesis genes in module M19 from 3- to 7-dpi, as well as the increase of growth-related genes in module M15, could be related to the attenuation of wound responses following apical bud clipping during inoculation, though a future study including an unwounded control would be required to investigate this.

4.3 | Induced responses differ between susceptible hosts

Responses in *P. greggii* indicated a loss of defence responses over time. While upregulated genes at 3-dpi included a few genes involved in auxin and JA signalling as well as a few *PR-16* genes, suggesting the presence of some defence responses, these responses were absent at 7-dpi. This could be associated with the downregulation of genes involved in transcription and translation at 3-dpi. The biotrophic smut fungus, *Ustilago maydis*, has been shown to successfully suppress host defences following penetration of the host dermis (Doehlemann et al., 2008). Swett et al. (2016) showed that *F. circinatum* is capable of biotrophically colonizing *P. radiata* roots, only resulting in tissue deterioration once the fungus reaches the root collar, suggesting the potential for a hemibiotrophic lifestyle. This gives rise to the possibility that the observed responses in *P. greggii* are the result of host defence suppression during biotrophic colonization.

While responses for resistant hosts show a lot of overlap, susceptible host responses show large variation. In contrast to the attenuation of responses observed for *P. greggii*, previously observed responses in *P. patula* suggested a delayed and compromised defence response, with less defence-related gene expression at 3-dpi and highly amplified responses at 7-dpi though key ET and JA signalling components, as well as a large complement of *R*-genes, were downregulated (Visser et al., 2019). Additionally, host responses to *F. circinatum* at 4-dpi in *P. radiata* showed upregulation of JA and ET biosynthesis genes, though a considerably higher number of JA and ET biosynthesis genes were upregulated in resistant *P. pinea* during the same trial, suggesting that the *P. radiata* response could be insufficient (Zamora-Ballesteros et al., 2021). Susceptibility to *F. circinatum* in *P. patula* could be further exacerbated by the higher constitutive expression of genes in module M06, many of which are involved in production of reactive oxygen species (ROS). Pathogen recognition in plants often triggers a hypersensitive response (HR), which includes ROS accumulation, resulting in localised cell death (reviewed in Barna et al., 2012). While this is an effective strategy against biotrophic pathogens, this often causes susceptibility against necrotrophs (Barna et al., 2012; Govrin & Levine, 2000). This suggests that susceptibility to *F. circinatum* challenge results from different failures in the induced responses of these three susceptible host species.

4.4 | Constitutive expression suggests predisposition to susceptibility

One possible explanation for the suppressed or missing JA/ET responses in susceptible relative to resistant hosts at 3-dpi could be antagonism by other phytohormone signalling pathways. Phytohormone crosstalk is complex and likely to be dosage dependent (Yang et al., 2015). The interaction between JA and SA signalling is usually classified as antagonistic (Naseem et al., 2015; Yang et al., 2015), though synergistic interactions also exist (Liu et al., 2016; Makandar et al., 2010). Furthermore, while JA-SA antagonism has been well described in angiosperms, current evidence suggests that this clearly defined antagonism only evolved after the angiosperm/gymnosperm split and additive roles for these hormones have been described in conifer defence responses (de Vries et al., 2018; Rigsby et al., 2019). Host responses in *P. tecunumanii*, as well as *P. oocarpa*, suggest that both these pathways play a role in host resistance (Visser et al., 2019). Module M11 suggested higher constitutive expression of certain SA-related innate immune responses in susceptible relative to resistant hosts. Although this module showed higher expression in inoculated relative to mock-inoculated samples from resistant hosts, further supporting a role for SA in host resistance, higher constitutive or wound responsive SA signalling in susceptible hosts could be detrimental to host resistance. Additionally, module M04, which showed higher expression in all susceptible relative to resistant samples, included genes involved in GA signalling. Increased cellular GA results in degradation of DELLA proteins,

attenuating JA signalling through the release of JAZ proteins (Hou et al., 2010).

Module M33 suggested higher constitutive cold stress responses in susceptible relative to resistant hosts. *P. patula* and *P. greggii* have been shown to have significantly higher frost tolerance compared to *P. tecunumanii* and *P. oocarpa* (Hodge et al., 2012). Interestingly, while high-elevation provenances of *P. tecunumanii* are more susceptible to *F. circinatum* compared to low-elevation provenances (Hodge & Dvorak, 2000), the high-elevation provenances have higher frost tolerance (Hodge et al., 2012). This gives rise to an issue in breeding programs, where hybrids might have increased *F. circinatum* resistance but decreased frost tolerance (Mitchell et al., 2013). Consequently, elucidating the genetic architecture of these responses would be invaluable to commercial pine forestry.

In conclusion, differences in both constitutive and induced expression between hosts have been implicated in host resistance and various points where resistance is effective against *F. circinatum* at the molecular level have been identified. These responses suggest that treatment with phytohormones to manipulate host defences or nutrient supplementation to improve sulfur metabolism could counteract compromised defences in susceptible hosts, leading to protection of seedlings. These are the next experiments to be explored.

ACKNOWLEDGEMENTS

The authors would like to thank South African Forestry Companies Limited (SAFCOL) and York Timbers for providing the plant material, Ms. Robyn Smith for assistance with the inoculation trials, and the Department of Science and Innovation (DSI), South Africa, Technology Innovation Agency (TIA), Forest Molecular Genetics cluster programme for funding the study.

CONFLICTS OF INTEREST

The authors declare no conflict of interest. The funders had no role in the design of the study; in the collection, analyses, or interpretation of data; in the writing of the manuscript, or in the decision to publish the results.

DATA AVAILABILITY STATEMENT

Sequence data supporting the findings of this study are available from the National Centre for Biotechnology Information (NCBI) BioProject data libraries under accession numbers: PRJNA416697 (*P. tecunumanii*), PRJNA416698 (*P. patula*), PRJNA685280 (*P. oocarpa*), PRJNA685282 (*P. maximinoi*), PRJNA685281 (*P. greggii*).

ORCID

Erik A. Visser http://orcid.org/0000-0002-4887-460X
Sanushka Naidoo http://orcid.org/0000-0001-5620-5599

REFERENCES

Agrios, G.N. (2005) *Plant pathology*, 5th edition. Academic Press.

Amaral, J., Lamelas, L., Valledor, L., Castillejo, M.Á., Alves, A. & Pinto, G. (2021) Comparative proteomics ofPinus–Fusariumcircinatuminteractions reveal metabolic clues to biotic stress resistance. *Physiologia Plantarum*, 173, 2142–2154. Available at https://doi.org/10.1111/ppl.13563

Andrews, S. (2010) *FastQC a quality control tool for high throughput sequence data*. http://www.bioinformatics.babraham.ac.uk/projects/fastqc/

Asiegbu, F.O., Choi, W., Li, G., Nahalkova, J. & Dean, R.A. (2003) Isolation of a novel antimicrobial peptide gene (Sp-AMP) homologue from *Pinus sylvestris* (Scots pine) following infection with the root rot fungus *Heterobasidion annosum*. *FEMS Microbiology Letters*, 228(1), 27–31. Available at https://doi.org/10.1016/s0378-1097(03)00697-9

Baggs, E., Dagdas, G. & Krasileva, K. (2017) NLR diversity, helpers and integrated domains: making sense of the NLR identity. *Current Opinion in Plant Biology*, 38, 59–67.

Barna, B., Fodor, J., Harrach, B.D., Pogány, M. & Király, Z. (2012) The Janus face of reactive oxygen species in resistance and susceptibility of plants to necrotrophic and biotrophic pathogens. *Plant Physiology and Biochemistry*, 59, 37–43. Available at https://doi.org/10.1016/j.plaphy.2012.01.014

Blande, D., Halimaa, P., Tervahauta, A.I., Aarts, M.G.M. & Kärenlampi, S.O. (2017) De novo transcriptome assemblies of four accessions of the metal hyperaccumulator plant *Noccaea caerulescens*. *Scientific Data*, 4, 160131. Available at https://doi.org/10.1038/sdata.2016.131

Bolger, A.M., Lohse, M. & Usadel, B. (2014) Trimmomatic: a flexible trimmer for illumina sequence data. *Bioinformatics*, 30, 2114–2120. Available at https://doi.org/10.1093/bioinformatics/btu170.

Bray, N.L., Pimentel, H., Melsted, P. & Pachter, L. (2016) Near-optimal probabilistic RNA-seq quantification. *Nature Biotechnology*, 34(5), 525–527. Available at https://doi.org/10.1038/nbt.3519

Buchfink, B., Xie, C. & Huson, D.H. (2014) Fast and sensitive protein alignment using DIAMOND. *Nature Methods*, 12(1), 59–60. Available at https://doi.org/10.1038/nmeth.3176

Capaldi, F.R., Gratão, P.L., Reis, A.R., Lima, L.W., & Azevedo, R.A. (2015). Sulfur metabolism and stress defense responses in plants. *Tropical Plant Biology*, 8(3–4), 60–73. https://doi.org/10.1007/s12042-015-9152-1

Carrasco, A., Wegrzyn, J.L., Durán, R., Fernández, M., Donoso, A. et al. (2017) Expression profiling in *Pinus radiata* infected with *Fusarium circinatum*. *Tree Genetics & Genomes*, 13, 46. Available at https://doi.org/10.1007/s11295-017-1125-0

Chong, J., Baltz, R., Schmitt, C., Beffa, R., Fritig, B. & Saindrenan, P. (2002) Downregulation of a pathogen-responsive tobacco UDP-Glc: Phenylpropanoid glucosyltransferase reduces scopoletin glucoside accumulation, enhances oxidative stress, and weakens virus resistance. *The Plant Cell*, 14(5), 1093–1107. Available at https://doi.org/10.1105/tpc.010436

Crous, J.W. (2005) Post establishment survival of *Pinus patula* in Mpumalanga, one year after planting. *The Southern African Forestry Journal*, 205, 3–11. Available at https://doi.org/10.2989/10295920509505232

Custers, J.H.H.V., Harrison, S.J., Sela-Buurlage, M.B., Van Deventer, E., Lageweg, W., Howe, P.W. et al. (2004) Isolation and characterisation of a class of carbohydrate oxidases from higher plants, with a role in active defence. *The Plant Journal*, 39, 147–160. Available at https://doi.org/10.1111/j.1365-313X.2004.02117.x

Dobin, A., Davis, C.A., Schlesinger, F., Drenkow, J., Zaleski, C., Jha, S. et al. (2013) STAR: ultrafast universal RNA-seq aligner. *Bioinformatics*, 29, 15–21. Available at https://doi.org/10.1093/bioinformatics/bts635

Dodds, P.N. & Rathjen, J.P. (2010) Plant immunity: towards an integrated view of plant–pathogen interactions. *Nature Reviews Genetics*, 11, 539–548. Available at https://doi.org/10.1038/nrg2812

Doehlemann, G., Wahl, R., Horst, R.J., Voll, L.M., Usadel, B., Poree, F. et al. (2008) Reprogramming a maize plant: transcriptional and metabolic changes induced by the fungal biotroph *Ustilago maydis*. *The Plant Journal*, 56, 181–195. Available at https://doi.org/10.1111/j.1365-313X.2008.03590.x

Donoso, A., Rodriguez, V., Carrasco, A., Ahumada, R., Sanfuentes, E. & Valenzuela, S. (2015) Relative expression of seven candidate genes for pathogen resistance on *Pinus radiata* infected with *Fusarium circinatum*. *Physiological and Molecular Plant Pathology*, 92, 42–50. Available at https://doi.org/10.1016/j.pmpp.2015.08.009

Dubuis, P.H., Marazzi, C., Stadler, E. & Mauch, F. (2005) Sulphur deficiency causes a reduction in antimicrobial potential and leads to increased disease susceptibility of oilseed rape. *Journal of Phytopathology*, 153(1), 27–36. Available at https://doi.org/10.1111/j.1439-0434.2004.00923.x

Dunwell, J.M., Gibbings, J.G., Mahmood, T. & Saqlan Naqvi, S.M. (2008) Germin and germin-like proteins: evolution, structure, and function. *Critical Reviews in Plant Sciences*, 27, 342–375. Available at https://doi.org/10.1080/07352680802333938

Dvorak, W. (2012) The strategic importance of applied tree conservation programs to the forest industry in South Africa. *Southern Forests: A Journal of Forest Science*, 74, 1–6. Available at https://doi.org/10.2989/20702620.2012.683635

Earle, C.J. *Pinus radiata*. The Gymnosperm Database. Available online: https://www.conifers.org/pi/Pinus_radiata.php [Accessed 17th January 2022].

Emms, D.M. & Kelly, S. (2015) OrthoFinder: solving fundamental biases in whole genome comparisons dramatically improves orthogroup inference accuracy. *Genome Biology*, 16, 157. Available at https://doi.org/10.1186/s13059-015-0721-2

Falcone Ferreyra, M.L., Rius, S.P. & Casati, P. (2012) Flavonoids: biosynthesis, biological functions, and biotechnological applications. *Frontiers in Plant Science*, 3, 222. Available at https://doi.org/10.3389/fpls.2012.00222

Falk, T., Herndon, N., Grau, E., Buehler, S., Richter, P., Zaman, S. et al. (2018) Growing and cultivating the forest genomics database, TreeGenes. *Database*, 2018, 1–11. Available at https://doi.org/10.1093/database/bay084

Fister, A.S., Mejia, L.C., Zhang, Y., Herre, E.A., Maximova, S.N. & Guiltinan, M.J. (2016) *Theobroma cacao* L. pathogenesis-related gene tandem array members show diverse expression dynamics in response to pathogen colonization. *BMC Genomics*, 17, 363. Available at https://doi.org/10.1186/s12864-016-2693-3

Van Ghelder, C., Parent, G.J., Rigault, P., Prunier, J., Giguère, I., Caron, S. et al. (2019) The large repertoire of conifer NLR resistance genes includes drought responsive and highly diversified RNLs. *Scientific Reports*, 9, 11614. Available at https://doi.org/10.1038/s41598-019-47950-7

Gilbert, D. (2013) Gene-omes built from mRNA seq not genome DNA. *7th annual arthropod genomics symposium, Notre Dame*. Available online: http://arthropods.eugenes.org/EvidentialGene/about/EvigeneRNA2013poster.pdf; http://globalhealth.nd.edu/7th-annual-arthropod-genomics-symposium/; https://doi.org/10.7490/f1000research.1112594.1

Gordon, T.R., Storer, A.J. & Wood, D.L. (2001) The pitch canker epidemic in California. *Plant Disease*, 85, 1128–1139. Available at https://doi.org/10.1094/PDIS.2001.85.11.1128

Gordon, T.R., Swett, C.L. & Wingfield, M.J. (2015) Management of *fusarium* diseases affecting conifers. *Crop Protection*, 73, 28–39. Available at https://doi.org/10.1016/j.cropro.2015.02.018

Govrin, E.M. & Levine, A. (2000) The hypersensitive response facilitates plant infection by the necrotrophic pathogen *Botrytis cinerea*. *Current Biology*, 10(13), 751–757. Available at https://doi.org/10.1016/S0960-9822(00)00560-1

Grabherr, M.G., Haas, B.J., Yassour, M., Levin, J.Z., Thompson, D.A., Amit, I. et al. (2011) Full-length transcriptome assembly from RNA-Seq data without a reference genome. *Nature Biotechnology*, 29, 644–652. Available at https://doi.org/10.1038/nbt.1883

Graham, T.L., Graham, M.Y., Subramanian, S. & Yu, O. (2007) RNAi silencing of genes for elicitation or biosynthesis of 5-deoxyisoflavonoids suppresses race-specific resistance and hypersensitive cell death in *Phytophthora sojae* infected tissues. *Plant Physiology*, 144(2), 728–740. Available at https://doi.org/10.1104/pp.107.097865

Grunewald, W., Vanholme, B., Pauwels, L., Plovie, E., Inzé, D., Gheysen, G. et al. (2009) Expression of thearabidopsisjasmonate signalling repressorJAZ1/TIFY10Ais stimulated by auxin. *EMBO Reports*, 10(8), 923–928. Available at https://doi.org/10.1038/embor.2009.103

Głowacki, S., Macioszek, V.K. & Kononowicz, A.K. (2011) R proteins as fundamentals of plant innate immunity. *Cellular & Molecular Biology Letters*, 16, 1–24. Available at https://doi.org/10.2478/s11658-010-0024-2

Hart, A.J., Ginzburg, S., Xu, M., Fisher, C.R., Rahmatpour, N., Mitton, J.B. et al. (2019) EnTAP: bringing faster and smarter functional annotation to non-model eukaryotic transcriptomes. *Molecular Ecology Resources*, 20(2), 591–604. Available at https://doi.org/10.1111/1755-0998.13106

Hepting, G.H. & Roth, E.R. (1946) Pitch canker, a new disease of some Southern pines. *Journal of Forestry*, 44, 742–744. Available at https://doi.org/10.1093/jof/44.10.742

Hernandez-Escribano, L., Visser, E.A., Iturritxa, E., Raposo, R. & Naidoo, S. (2020) The transcriptome of *Pinus pinaster* under *Fusarium circinatum* challenge. *BMC Genomics*, 21, 28. Available at https://doi.org/10.1186/s12864-019-6444-0

Hill, C.B., Cassin, A., Keeble-Gagnère, G., Doblin, M.S., Bacic, A. & Roessner, U. (2016) De novo transcriptome assembly and analysis of differentially expressed genes of two barley genotypes reveal root-zone-specific responses to salt exposure. *Scientific Reports*, 6, 31558. Available at https://doi.org/10.1038/srep31558

Hodge, G.R., Dvorak, W.S. & Tighe, M. (2012) Comparisons between laboratory and field results of frost tolerance of pines from the Southern USA and Mesoamerica planted as exotics. *Southern Forests: A Journal of Forest Science*, 74(1), 7–17. Available at https://doi.org/10.2989/20702620.2012.683637

Hodge, G.R. & Dvorak, W.S. (2000) Differential responses of central American and Mexican pine species and *Pinus radiata* to infection by the pitch canker fungus. *New Forests*, 19, 241–258. Available at https://doi.org/10.1023/A:1006613021996

Hodge, G.R. & Dvorak, W.S. (2007) Variation in pitch canker resistance among provenances of *Pinus patula* and *Pinus tecunumanii* from Mexico and Central America. *New Forests*, 33, 193–206. Available at https://doi.org/10.1007/s11056-006-9023-6

Hou, X., Lee, L.Y.C., Xia, K., Yan, Y. & Yu, H. (2010) DELLAs modulate jasmonate signaling via competitive binding to JAZs. *Developmental Cell*, 19(6), 884–894. Available at https://doi.org/10.1016/j.devcel.2010.10.024

Huerta-Cepas, J., Szklarczyk, D., Forslund, K., Cook, H., Heller, D., Walter, M.C. et al. (2016) Eggnog 4.5: a hierarchical orthology framework with improved functional annotations for eukaryotic, prokaryotic and viral sequences. *Nucleic Acids Research*, 44, D286–D293. Available at https://doi.org/10.1093/nar/gkv1248

Huot, B., Yao, J., Montgomery, B.L. & He, S.Y. (2014) Growth-defense tradeoffs in plants: a balancing act to optimize fitness. *Molecular Plant*, 7(8), 1267–1287. Available at https://doi.org/10.1093/mp/ssu049

Ibraheem, F., Gaffoor, I. & Chopra, S. (2010) Flavonoid phytoalexin-dependent resistance to anthracnose leaf blight requires a functional yellow seed 1 in Sorghum bicolor. *Genetics*, 184, 915–926. Available at https://doi.org/10.1534/genetics.109.111831

Jackson, C., Christie, N., Reynolds, S.M., Marais, G.C., Tii-kuzu, Y., Caballero, M. et al. (2021) A genome-wide SNP genotyping resource for tropical pine tree species. *Molecular Ecology Resources*, 22, 695–710. Available at https://doi.org/10.1111/1755-0998.13484

Jones, J.D.G. & Dangl, J.L. (2006) The plant immune system. *Nature*, 444, 323–429. Available at https://doi.org/10.1038/nature05286

Kanehisa, M., Sato, Y. & Morishima, K. (2016) BlastKOALA and GhostKOALA: KEGG tools for functional characterization of genome and metagenome sequences. *Journal of Molecular Biology*, 428(4), 726–731. Available at https://doi.org/10.1016/j.jmb.2015.11.006

Keeling, C.I. & Bohlmann, J. (2006) Genes, enzymes and chemicals of terpenoid diversity in the constitutive and induced defence of conifers against insects and pathogens*. *New Phytologist*, 170, 657–675. Available at https://doi.org/10.1111/j.1469-8137.2006.01716.x

Kubisiak, T.L., Amerson, H.V. & Nelson, C.D. (2005) Genetic interaction of the fusiform rust fungus with resistance gene *Fr1* in loblolly pine. *Phytopathology®*, 95, 376–380. Available at https://doi.org/10.1094/PHYTO-95-0376

Langfelder, P. & Horvath, S. (2008) WGCNA: an R package for weighted correlation network analysis. *BMC Bioinformatics*, 9, 559. Available at https://doi.org/10.1186/1471-2105-9-559

Langfelder, P. & Horvath, S. (2012) Fast R functions for robust correlations and hierarchical clustering. *Journal of Statistical Software*, 46(11), 1–17.

Leek, J.T., Johnson, W.E., Parker, H.S., Fertig, E.J., Jaffe, A.E. et al. (2019) sva: surrogate variable analysis. R package version 3.34.0.

Liu, L., Sonbol, F.M., Huot, B., Gu, Y., Withers, J., Mwimba, M. et al. (2016) Salicylic acid receptors activate jasmonic acid signalling through a non-canonical pathway to promote effector-triggered immunity. *Nature Communications*, 7, 13099. Available at https://doi.org/10.1038/ncomms13099

Lohse, M., Nagel, A., Herter, T., May, P., Schroda, M., Zrenner, R. et al. (2014) Mercator: a fast and simple web server for genome scale functional annotation of plant sequence data. *Plant, Cell & Environment*, 37(5), 1250–1258. Available at https://doi.org/10.1111/pce.12231

Love, M.I., Huber, W. & Anders, S. (2014) Moderated estimation of fold change and dispersion for RNA-seq data with DESeq. 2. *Genome Biology*, 15(12), 550. Available at https://doi.org/10.1186/s13059-014-0550-8

Maffei, M.E., Gertsch, J. & Appendino, G. (2011) Plant volatiles: production, function and pharmacology. *Natural Product Reports*, 28, 1359–1380. Available at https://doi.org/10.1039/c1np00021g

Makandar, R., Nalam, V., Chaturvedi, R., Jeannotte, R., Sparks, A.A. & Shah, J. (2010) Involvement of salicylate and jasmonate signaling pathways in *Arabidopsis* interaction with *Fusarium graminearum*. *Molecular Plant-Microbe Interactions®*, 23(7), 861–870. Available at https://doi.org/10.1094/MPMI-23-7-0861

Manners, J.M. (2009) Primitive defence: the MiAMP1 antimicrobial peptide family. *Plant Molecular Biology Reporter*, 27, 237–242. Available at https://doi.org/10.1007/s11105-008-0083-y

Marcus, J.P., Goulter, K.C., Green, J.L., Harrison, S.J. & Manners, J.M. (1997) Purification, characterisation and cDNA cloning of an antimicrobial peptide from *Macadamia integrifolia*. *European Journal of Biochemistry*, 244, 743–749. Available at https://doi.org/10.1111/j.1432-1033.1997.00743x

Mitchell, R.G., Steenkamp, E., Coutinho, T. & Wingfield, M. (2011) The pitch canker fungus, *Fusarium circinatum*: implications for South African forestry. *Southern Forests: a Journal of Forest Science*, 73, 1–13. Available at https://doi.org/10.2989/20702620.2011.574828

Mitchell, R.G., Wingfield, M.J., Hodge, G.R., Steenkamp, E.T. & Coutinho, T.A. (2012) Selection of *Pinus* spp. in South Africa for tolerance to infection by the pitch canker fungus. *New Forests*, 43, 473–489. Available at https://doi.org/10.1007/s11056-011-9293-5

Mitchell, R.G., Wingfield, M.J., Hodge, G.R., Steenkamp, E.T. & Coutinho, T.A. (2013) The tolerance of *Pinus patula*× *Pinus tecunumanii*, and other pine hybrids, to *Fusarium circinatum* in greenhouse trials. *New Forests*, 44, 443–456. Available at https://doi.org/10.1007/s11056-012-9355-3

Moraga-Suazo, P., Orellana, L., Quiroga, P., Balocchi, C., Sanfuentes, E., Whetten, R.W. et al. (2014) Development of a genetic linkage map for *Pinus radiata* and detection of pitch canker disease resistance associated QTLs. *Trees*, 28, 1823–1835. Available at https://doi.org/10.1007/s00468-014-1090-2

Morse, A.M., Nelson, C.D., Covert, S.F., Holliday, A.G., Smith, K.E. & Davis, J.M. (2004) Pine genes regulated by the necrotrophic pathogen *Fusarium circinatum*. *Theoretical and Applied Genetics*, 109, 922–932. Available at https://doi.org/10.1007/s00122-004-1719-4

Naseem, M., Kaltdorf, M. & Dandekar, T. (2015) The nexus between growth and defence signalling: auxin and cytokinin modulate plant immune response pathways. *Journal of Experimental Botany*, 66(16), 4885–4896. Available at https://doi.org/10.1093/jxb/erv297

Nirenberg, H.I. & O'Donnell, K. (1998) New *fusarium* species and combinations within the *Gibberella fujikuroi* species complex. *Mycologia*, 90, 434–458. Available at https://doi.org/10.1080/00275514.1998.12026929

Nurnberger, T. & Kemmerling, B. (2009) PAMP-Triggered basal immunity in plants. In: van Loon, L.C., (ed) *Advances in Botanical Research – Plant Innate Immunity*. Oxford, UK: Elsevier Ltd. pp. 1–38.

Nürnberger, T. & Lipka, V. (2005) Non-host resistance in plants: new insights into an old phenomenon. *Molecular Plant Pathology*, 6, 335–345. Available at https://doi.org/10.1111/j.1364-3703.2005.00279.x

Quesada, T., Gopal, V., Cumbie, W.P., Eckert, A.J., Wegrzyn, J.L., Neale, D.B. et al. (2010) Association mapping of quantitative disease resistance in a natural population of loblolly pine (*Pinus taeda* L.). *Genetics*, 186, 677–686. Available at https://doi.org/10.1534/genetics.110.117549

Quesada, T., Resende M. Jr., Muñoz, P., Wegrzyn, J., Neale, D., Kirst, M. et al. (2014) Mapping fusiform rust resistance genes within a complex mating design of loblolly pine. *Forests*, 5, 347–362. Available at https://doi.org/10.3390/f5020347

R Core Team (2019) *R: a language and environment for statistical computing*. Vienna, Austria: R Foundation for Statistical Computing. https://www.R-project.org/

Reijnders, M.J.M.F. & Waterhouse, R.M. (2021) Summary visualizations of gene ontology terms with GO-figure! *Frontiers in Bioinformatics*, 1, 6. Available at https://doi.org/10.3389/fbinf.2021.638255

Richard, S., Lapointe, G., Rutledge, R.G. & Séguin, A. (2000) Induction of chalcone synthase expression in white spruce by wounding and jasmonate. *Plant and Cell Physiology*, 41(8), 982–987. Available at https://doi.org/10.1093/pcp/pcd017

Rigsby, C.M., Shoemaker, E.E., Mallinger, M.M., Orians, C.M. & Preisser, E.L. (2019) Conifer responses to a stylet-feeding invasive herbivore and induction with methyl jasmonate: impact on the expression of induced defences and a native folivore. *Agricultural and Forest Entomology*, 21(2), 227–234. Available at https://doi.org/10.1111/afe.12324

Robertson, G., Schein, J., Chiu, R., Corbett, R., Field, M., Jackman, S.D. et al. (2010) *De novo* assembly and analysis of RNA-seq data. *Nature Methods*, 7, 909–912. Available at https://doi.org/10.1038/nmeth.1517

Roux, J., Eisenberg, B., Kanzler, A., Nel, A., Coetzee, V., Kietzka, E. et al. (2007) Testing of selected South African *Pinus* hybrids and families for tolerance to the pitch canker pathogen, *Fusarium circinatum*. *New Forests*, 33, 109–123. Available at https://doi.org/10.1007/s11056-006-9017-4

Shannon, P., Markiel, A., Ozier, O., Baliga, N.S., Wang, J.T., Ramage, D. et al. (2003) Cytoscape: a software environment for integrated models of biomolecular interaction networks. *Genome Research*, 13, 2498–2504. Available at https://doi.org/10.1101/gr.1239303

Simão, F.A., Waterhouse, R.M., Ioannidis, P., Kriventseva, E.V. & Zdobnov, E.M. (2015) BUSCO: assessing genome assembly and annotation completeness with single-copy orthologs. *Bioinformatics*, 31(19), 3210–3212. Available at https://doi.org/10.1093/bioinformatics/btv351

Smith-Unna, R., Boursnell, C., Patro, R., Hibberd, J.M. & Kelly, S. (2016) TransRate: reference-free quality assessment of *de novo* transcriptome assemblies. *Genome Research*, 26, 1134–1144. Available at https://doi.org/10.1101/gr.196469.115

Soneson, C., Love, M.I. & Robinson, M.D. (2015) Differential analyses for RNA-seq: transcript-level estimates improve gene-level inferences. *F1000Research*, 4, 1521. Available at https://doi.org/10.12688/f1000research.7563.2

Sooriyaarachchi, S., Jaber, E., Covarrubias, A.S., Ubhayasekera, W., Asiegbu, F.O. & Mowbray, S.L. (2011) Expression and β-glucan binding properties of Scots pine (*Pinus sylvestris* L.) antimicrobial protein (Sp-AMP). *Plant Molecular Biology*, 77, 33–45. Available at https://doi.org/10.1007/s11103-011-9791-z

Spoel, S.H. & Dong, X. (2012) How do plants achieve immunity? defence without specialized immune cells. *Nature Reviews Immunology*, 12(2), 89–100. Available at https://doi.org/10.1038/nri3141

Swett, C.L., Kirkpatrick, S.C. & Gordon, T.R. (2016) Evidence for a hemibiotrophic association of the pitch canker pathogen *Fusarium circinatum* with *Pinus radiata*. *Plant Disease*, 100, 79–84. Available at https://doi.org/10.1094/PDIS-03-15-0270-RE

Tang, S., Lomsadze, A. & Borodovsky, M. (2015) Identification of protein coding regions in RNA transcripts. *Nucleic Acids Research*, 43, e78. Available at https://doi.org/10.1093/nar/gkv227

Thimm, O., Bläsing, O., Gibon, Y., Nagel, A., Meyer, S., Krüger, P. et al. (2004) MAPMAN: a user-driven tool to display genomics data sets onto diagrams of metabolic pathways and other biological processes. *The Plant Journal*, 37(6), 914–939. Available at https://doi.org/10.1111/j.1365-313X.2004.02016.x

Treutter, D. (2006) Significance of flavonoids in plant resistance: a review. *Environmental Chemistry Letters*, 4, 147–157. Available at https://doi.org/10.1007/s10311-006-0068-8

VanBel, M., Diels, T., Vancaester, E., Kreft, L., Botzki, A., Van de Peer, Y. et al. (2017) PLAZA 4.0: an integrative resource for functional, evolutionary and comparative plant genomics. *Nucleic Acids Research*, 46, D1190–D1196. Available at https://doi.org/10.1093/nar/gkx1002

Vettraino, A., Potting, R. & Raposo, R. (2018) EU legislation on forest plant health: an overview with a focus on *Fusarium circinatum*. *Forests*, 9, 568. Available at https://doi.org/10.3390/f9090568.

Visser, E.A., Wegrzyn, J.L., Myburg, A.A. & Naidoo, S. (2018) Defence transcriptome assembly and pathogenesis-related gene family analysis in *Pinus tecunumanii* (low elevation). *BMC Genomics*, 19(1), 632. Available at https://doi.org/10.1186/s12864-018-5015-0

Visser, E.A., Wegrzyn, J.L., Steenkamp, E.T., Myburg, A.A. & Naidoo, S. (2019) Dual RNA-seq analysis of the pine-*Fusarium circinatum* interaction in resistant (*Pinus tecunumanii*) and susceptible (*Pinus patula*) hosts. *Microorganisms*, 7(9), 315. Available at https://doi.org/10.3390/microorganisms7090315

Visser, E.A., Wegrzyn, J.L., Steenkmap, E.T., Myburg, A.A. & Naidoo, S. (2015) Combined de novo and genome guided assembly and annotation of the *Pinus patula* juvenile shoot transcriptome. *BMC Genomics*, 16(1), 1057. Available at https://doi.org/10.1186/s12864-015-2277-7

de Vries, S., de Vries, J., von Dahlen, J.K., Gould, S.B., Archibald, J.M., Rose, L.E. et al. (2018) On plant defense signaling networks and early land plant evolution. *Communicative & Integrative Biology*, 11(3), 1–14. Available at https://doi.org/10.1080/19420889.2018.1486168

Waterhouse, R.M., Seppey, M., Simão, F.A., Manni, M., Ioannidis, P., Klioutchnikov, G. et al. (2017) BUSCO applications from quality assessments to gene prediction and phylogenomics. *Molecular Biology and Evolution*, 35(3), 543–548. Available at https://doi.org/10.1093/molbev/msx319

Wegrzyn, J.L., Liechty, J.D., Stevens, K.A., Wu, L.S., Loopstra, C.A., Vasquez-Gross, H.A. et al. (2014) Unique features of the loblolly pine (*Pinus taeda* L.) megagenome revealed through sequence annotation. *Genetics*, 196, 891–909. Available at https://doi.org/10.1534/genetics.113.159996

Wegrzyn, J.L., Staton, M.A., Street, N.R., Main, D., Grau, E., Herndon, N. et al. (2019) Cyberinfrastructure to improve forest health and productivity: the role of tree databases in connecting genomes, phenomes, and the environment. *Frontiers in Plant Science*, 10, 813. Available at https://doi.org/10.3389/fpls.2019.00813

Wilcox, P.L., Amerson, H.V., Kuhlman, E.G., Liu, B.H., O'Malley, D.M. & Sederoff, R.R. (1996) Detection of a major gene for resistance to fusiform rust disease in loblolly pine by genomic mapping. *Proceedings of the National Academy of Sciences*, 93, 3859–3864. Available at https://doi.org/10.1073/pnas.93.9.3859

Wingfield, B.D., Steenkamp, E.T., Santana, Q.C., Coetzee, M.P.A., Bam, S., Barnes, I. et al. (2012) First fungal genome sequence from Africa: a preliminary analysis. *South African Journal of Science*, 108(1/2), 1–9. Available at https://doi.org/10.4102/sajs.v108i1/2.537

Wingfield, M.J., Hammerbacher, A., Ganley, R.J., Steenkamp, E.T., Gordon, T.R., Wingfield, B.D. et al. (2008) Pitch canker caused by *Fusarium circinatum*–a growing threat to pine plantations and forests worldwide. *Australasian Plant Pathology*, 37, 319–334. Available at https://doi.org/10.1071/AP08036

Yang, Y.X., Ahammed, G.J., Wu, C., Fan, S.Y. & Zhou, Y.H. (2015) Crosstalk among jasmonate, salicylate and ethylene signaling pathways in plant disease and immune responses. *Current Protein & Peptide Science*, 16(5), 450–461. Available at https://doi.org/10.2174/1389203716666150330141638

Young, M.D., Wakefield, M.J., Smyth, G.K. & Oshlack, A. (2010) Gene ontology analysis for RNA-seq: accounting for selection bias. *Genome Biology*, 11(2), R14. Available at https://doi.org/10.1186/gb-2010-11-2-r14

Yuan, H., Zeng, X., Yang, Q., Xu, Q., Wang, Y., Jabu, D. et al. (2018) Gene coexpression network analysis combined with metabonomics reveals the resistance responses to powdery mildew in Tibetan hulless barley. *Scientific Reports*, 8, 14928. Available at https://doi.org/10.1038/s41598-018-33113-7

Zamora-Ballesteros, C., Pinto, G., Amaral, J., Valledor, L., Alves, A., Diez, J.J. et al. (2021) Dual RNA-sequencing analysis of resistant (*Pinus pinea*) and susceptible (*Pinus radiata*) hosts during *Fusarium circinatum* challenge. *International Journal of Molecular Sciences*, 22(10), 5231. Available at https://doi.org/10.3390/ijms22105231

Zhou, N., Tootle, T.L., Tsui, F., Klessig, D.F. & Glazebrook, J. (1998) PAD4 functions upstream from salicylic acid to control defense responses in Arabidopsis. *The Plant Cell*, 10(6), 1021–1030. Available at https://doi.org/10.1105/tpc.10.6.1021.

Zulak, K.G. & Bohlmann, J. (2010) Terpenoid biosynthesis and specialized vascular cells of conifer defense. *Journal of Integrative Plant Biology*, 52, 86–97. Available at https://doi.org/10.1111/j.1744-7909.2010.00910.x

SUPPORTING INFORMATION

Additional supporting information can be found online in the Supporting Information section at the end of this article.

How to cite this article: Visser, E.A., Kampmann, T.P., Wegrzyn, J.L. & Naidoo, S. (2023) Multispecies comparison of host responses to *Fusarium circinatum* challenge in tropical pines show consistency in resistance mechanisms. *Plant, Cell & Environment*, 46, 1705–1725. https://doi.org/10.1111/pce.14522